FRACTURE IN ASPHALTIC MIXTURES

BY

WILLIAM WILSON KAKEL
SB, United States Military Academy
(1966)

Submitted in partial fulfillment

of the requirements for the degree of

Master of Science in Civil Engineering

at the

Massachusetts Institute of Technology

(1968)

Signature of Author . . . . . .
Department of Civil Engineering, 15 January 1968

Certified by . . . . . .
Thesis Supervisor

Accepted by . . . . . .
Chairman, Departmental Committee on Graduate Students

ABSTRACT

FRACTURE IN ASPHALTIC MIXTURES

by

WILLIAM WILSON KAKEL

Submitted to the Department of Civil Engineering on 15 January 1968, in partial fulfillment of the requirements for the degree of Master of Science in Civil Engineering.

The Griffith theory of brittle fracture is applied to asphalt and asphaltic mixtures in order to determine the effect of different variables on the fracture behavior of asphalt and to investigate possible means of improving the fracture toughness of asphalt at low temperatures. The critical strain-energy release rate is measured by simple bending tests on notched asphaltic beams. Two paving asphalts, coded B-2960 and B-3056, are tested at various conditions of aging, percentage of mineral filler, temperature, test environment, and rate of loading. The results of this study indicate that the addition of mineral filler increases the fracture toughness of asphalt threefold. The fracture behavior of asphalt and asphaltic mixtures is related to the fracture behavior of other polymeric materials.

Thesis Supervisor: Fred Moavenzadeh, Ph. D.

Title: Associate Professor of Civil Engineering

ACKNOWLEDGEMENTS

I wish to express my sincere appreciation to Dr. Fred Moavenzadeh for his invaluable advise and constant direction without which this thesis could not have been completed.

I wish to acknowledge Mr. Arthur Rudolph for his encouragement and his worthy supervision in the design and manufacture of much of the equipment used in this study.

Final thanks are due my mother for her help in typing this thesis and my wife for her patience, understanding, and constant support.

TABLE OF CONTENTS

TABLE OF CONTENTS (Continued)

INTRODUCTION

The problem of designing and constructing a highway pavement capable of withstanding the destructive effects of anticipated traffic loadings and weather conditions, in addition to providing riding qualities satisfactory to the highway user, is continually confronting the highway engineer. The analysis of the types of pavement failures and of the causes of these failures is an important step in the solution of this problem. This type of analysis has revealed that more knowledge must be gained in the area of material behavior: both, in determining characteristic properties of the paving materials which will better predict material behavior under varying conditions, and in developing means to improve these material properties so that the ultimate goal of better pavement performance can be attained.

The failure of asphalt paving mixtures is generally divided into three broad categories (1)*: instability, disintegration, and fracture or cracking. Some of the factors included in disintegration, such as low tensile strength and brittleness of the asphalt binder, are also, at least indirectly, related to fracture phenomena. Cracking in asphalt paving mixtures is primarily caused by thermal contraction and/or brittleness of the asphalt binder. Slippage between pavement layers,

---

*Numbers in parenthesis refer to References.

which likewise involves binder strength, also causes cracking failures. Consequently, the quantity and quality of the asphaltic binder and the change in its characteristics over the service life of the pavement are found to have considerable influence on cracking failures in the pavement. However, as yet there has been no direct consideration of the fracture strength of the asphalt binder in asphalt paving mix design requirements (2).

Cracks are primarily developed in the asphaltic mixture at low temperatures when asphalt becomes a brittle, glassy material. Cracking usually occurs either in the asphalt or at the interface between asphalt and aggregates. Brittle fracture theories have been applied to asphaltic materials when they exhibit brittle behavior under low temperature conditions (3). It was determined that the critical strain-energy release rate, G , can be calculated for asphalts, and that it appears to be a material property which would be useful in studying the fracture behavior of asphalts. Thus it seems reasonable that further investigations in this area would lead to a better understanding of cracking or fracture failures of asphalt paving mixtures and to ways of improving asphalt pavement performance.

An investigation of the fracture behavior of two paving asphalts is made in this study. Mineral filler has been added to the asphalts in an attempt to improve their fracture

toughness. Results of this study indicate that the addition of mineral filler to form asphaltic mixtures does significently improve the fracture toughness of asphalt.

REVIEW OF LITERATURE

This section briefly reviews the theory of brittle fracture and the applications that have been made of this theory to polymeric materials. The method of determining the critical strain-energy release rate used in this study is also discussed.

General Considerations of Fracture and Strength

The aim of theories of brittle fracture is to account for the discrepancy between the observed strength of materials as measured in conventional tests and the theoretical strength as predicted from the assumed molecular structure. The theoretical strength of an elastic material is determined from the forces of atomic bonds within the material. The fracture of the material under stress involves the rupture of those bonds which intersect the plane defined by the growing fracture surface. However, materials commonly fracture at applied stress levels 10 to 100 times below their theoretical atomic bond strengths.

The explanation for this discrepancy is that the experimental samples are not physically perfect; structural imperfections arise either as a result of the nature of the material, as in crystal defects, or as a result of mechanical handling or fabrication procedures, e.g. cracks and scratches. Therefore, the assumption, implicit in the

theoretical analysis, that the stress due to the applied load is distributed uniformly throughout the sample is not correct. The presence of these flaws locally affects the stress distribution in the body and reduces the imposed stress for fracture from the theoretical to the observed value. In an isotropic medium, the failure point is reached when the largest defect increases in size. Two approaches are possible to define the condition of stress at which this occurs.

Flaws in the material act as stress concentrators and thereby produce local stresses in the vicinity of the flaw which are much higher than the average value throughout the body. When the applied load is increased, the stresses at these points reach a limiting value corresponding to the "true" strength of the material, which is turn is related to interatomic bond strengths, while the average stress is still comparatively low. Local failure will then occur causing an increase in the size of the defect which results in further increases in local stress until the system becomes unstable and fracture occurs.

Alternatively, the thermodynamics of the process may be considered; the criterion for failure being defined in terms of the conditions under which the total energy of the (conservative) system decreases with increasing flaw size. Since the system is conservative, allowance must be

made for the work done on the system by the imposed stress as the external boundaries are displaced. This external work on the system is converted into fracture surface energy as the flaw increases in size.

Griffith Theory of Brittle Fracture

A satisfactory explanation of brittle strength phenomena utilizing the thermodynamic approach was first proposed by Griffith (4, 5). His analysis was partly based on the earlier work of Inglis (6), who had analyzed the elastic stress distribution around an elliptical hole in a stressed plate utilizing the classical methods of elasticity.

Inglis, for an infinite plate of unit thickness containing a very flat elliptical hole with a major axis of length 2c perpendicular to a stress field, σ, applied at the edges of the plate, determined that the maximum tensile stress would occur at the ends of the major axis and would be equal to:

$$\sigma_m = 2\sigma (c/\rho)^{1/2} \qquad \text{Equation 1}$$

where σ_m is the maximum tensile stress which occurs in the vicinity of the crack, and ρ is the radius of curvature at the ends of the major axis of the hole, or crack. If it is assumed that the material would fail for some critical value of σ_m, then as ρ approached zero, the value of σ required to cause failure would also approach zero due to

this infinite singularity in the stress field. However, such is not the case; for even with the sharpest cracks, there is still an appreciable value of tensile strength present upon failure.

The presence of tensile strength when the crack tip radius approaches zero was explained by Griffith using the concept of surface energy and the principle of the conservation of energy.. Two contributions to the energy of the system were considered: the elastic strain energy of the system U, and the surface energy T. The former arises from the work done on the system by the imposed stresses, while the latter arises from the energy required for the formation of the fracture surfaces as the original defect increases in size.

Griffith assumed that the defect was a line crack $(\rho \to 0)$ of length 2c and determined that, for the case of plane stress, the excess strain energy of the cracked plate described by Inglis over that of a plate without a crack would be

$$\Delta U = \frac{\pi c^2 \sigma^2}{E} \qquad \text{Equation 2}$$

per unit thickness of the plate. The work done in creating new surface energy as the crack extends is given as

$$\Delta T = 4\gamma c \qquad \text{Equation 3}$$

per unit thickness of the plate, where γ is the surface energy of the material per unit area. The factor of four is

present due to the fact that two surfaces are being created at each end of the crack as the crack propagates.

Griffith further postulated that the crack would lengthen and cause gross fracture if, for a small increase of its length, the release in elastic strain energy became equal to the energy required to form new surfaces, that is, if

$$\frac{d\Delta W}{dc} = \frac{d(\Delta T - \Delta U)}{dc} = 0$$

$$\frac{\pi c \sigma^2}{E} = 2\gamma$$

applying this criterion, the critical stress for failure is found to be

$$\sigma = \sqrt{\frac{2\gamma E}{\pi c}} \qquad \text{Equation 4}$$

which is the well-known Griffith formula. For the case of plane strain (thick plate), E must be replaced by $E/(1-\nu^2)$ and Equation 4 becomes

$$\sigma = \sqrt{\frac{2\gamma E}{\pi(1-\nu^2)c}} \qquad \text{Equation 5}$$

where ν is the Poisson's ratio of the material.

Verification of this work by Griffith has been made by several investigators including Griffith (4) and others as discussed by Orowan (7) for various materials. They have confirmed that the presence of very small cracks greatly reduce the measured tensile strengths of materials which fail in a brittle fashion. Furthermore, it was found (7) that surface cracks are usually most critical in the process of brittle failure.

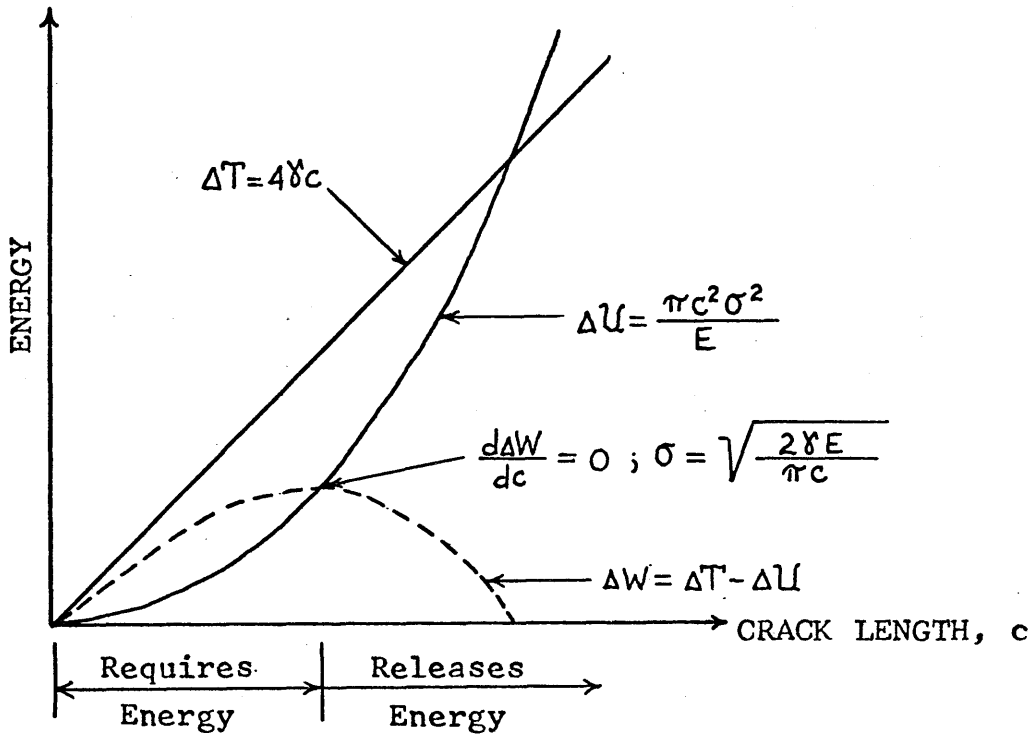

Figure 1 - The Griffith Case

Modifications of Griffith's Theory

During World War II the Griffith criterion was applied to the brittle fracture of ship steel. However, it was found (8) that the measured surface energy was 1,000 times greater than the theoretical estimate based only on the reversible work necessary to separate two atomic planes of the metal. Orowan (8) and Irwin (9) attributed this large discrepancy to the formation of a plastically deformed region of material near the tip of the crack which absorbs a large amount of

irreversible work during the crack propagation. They suggested that, for materials in which plastic flow is present before the onset of brittle fracture, Griffith's formula in a modified form could be used as long as the plastic strains tended to localize near the boundaries of the crack. In this case, the term for surface energy in Equations 4 and 5 must be replaced by a term that includes the work of the plastic strains as well as the work of creating new surface energy. Therefore, the modified Griffith version of Equation 4 becomes

$$\sigma = \sqrt{\frac{2\gamma_p E}{\pi c}} \qquad \text{Equation 6}$$

where γ_p is the sum of all the work done in propagating the crack. γ_p is referred to as the surface work term. Orowan showed by means of x-ray diffraction studies that the plastic work portion of γ_p is orders of magnitude larger than the surface energy portion for most metals.

Another modification of Griffith's work was suggested by Irwin (10). In the Griffith theory the strain energy derivative is equated to the surface energy derivative in the instability criterion to give the value of the critical imposed stress for failure. However, Irwin does not equate the strain energy derivative to the surface energy derivative since the former term includes all contributions to the energy dissipated as the crack advances, including those which

are not related directly to that required for the formation of new surface area. Thus, Irwin proposed that the strain-energy release rate, which can be determined by taking the derivative of Equation 2 to give

$$G = \frac{dU}{dc} = \frac{2\pi c\sigma^2}{E} \qquad \text{Equation 7}$$

for the case of plane stress, is the true driving force in crack propagation. The value of the strain-energy release rate at the onset of unstable crack propagation is referred to as the critical strain-energy release rate, Gc. This is equal to 2γ in Griffith's equation. Irwin also suggested (11) that, since different loading conditions could produce the same stress concentration at the tip of the crack, this critical value of the strain-energy release rate would be a constant for the material, such as the modulus of elasticity, E, is a constant for the material.

Limiting Local Stress Criterion For Fracture

The Griffith theory and its modifications considered the condition of instability for brittle fracture from the thermodynamic viewpoint. As stated previously, a second criterion which may be adopted is that fracture initiates when the concentrated stress at the tip of the crack reaches a particular limiting value corresponding to the true strength of the material.

Inglis (6) determined that the maximum stress would

occur at the tip of the crack and would be equal to

$$\sigma_m = 2\sigma (c/\rho)^{1/2} \qquad \text{Equation 1}$$

Orowan (7) pointed out that, physically, the minimum radius of curvature at the tip of the crack is of the order of magnitude of the interatomic spacing, a. Thus, if in Equation 1, ρ is replaced by a, and σ_m is equated to the theoretical or "true" strength of the material (7) given by

$$\sigma_c = \sqrt{\frac{2\gamma E}{a}} \qquad \text{Equation 8}$$

the value of the applied mean stress, at which the microscopic stress at a crack of atomic sharpness reaches the value of the molecular cohesion, would be

$$2\sigma\sqrt{\frac{c}{a}} = \sqrt{\frac{2\gamma E}{a}}$$

or

$$\sigma = \sqrt{\frac{\gamma E}{2c}} \qquad \text{Equation 9}$$

The stress required for fracture obtained by the Griffith theory is

$$\sigma = \sqrt{\frac{2\gamma E}{\pi c}} \qquad \text{Equation 4}$$

The difference in the two values is relatively small and is well within the accuracy of assumptions made in the Griffith theory, (e.g. the use of Hooke's law up to the moment of fracture).

Application of Fracture Theories to Polymeric Materials

With regards to their macroscopic mechanical properties, amorphous polymeric materials, materials composed of long chain molecules arranged in random array, essentially behave as elastic bodies under those conditions where they display a brittle mode of fracture. Furthermore, on a macroscopic scale, glassy amorphous polymers frequently are isotropic. Consequently, it is reasonable to apply to these materials the theories of brittle fracture which have been derived from consideration of classically elastic models.

Amorphous polymers display brittle behavior when tested below their glass transition temperature. Below this temperature there is a decrease in the material's expansion coefficient and its molecular structure is effectively fixed. Above the glass transition temperature, viscoelastic behavior occurs and fracture behavior becomes more sensitive to strain rate and temperature. If temperatures are not kept low enough to maintain the polymer in a glassy state, significent macroscopic inelastic response in the samples results, which invalidates the application of brittle fracture theories to these materials.

Brittle fracture theories have been applied to polymeric materials (12, 13). Cleavage tests were used to calculate the fracture surface works γ_p , the energy required for the formation of new surfaces by the extension of the

critical flaw. The experimentally determined fracture surface work for Plexiglas (poly-methylmethacrylate or PMMA) and polystyrene, the primary polymers tested, were both nearly 1,000 times greater than the theoretical value of surface energy for glassy polymers calculated on the premise that only primary, covalent bonds of the carbon-carbon polymer chain in molecules oriented normal to the crack are ruptured during the fracture process. This large discrepancy is similar to that observed for ship steel (see Table 1) and, likewise, is attributed to the energy dissipated in inelastic processes which occur under the influence of the high stresses at the tip of the flaw. Thus, despite the fact that macroscopically the fracture behavior of polymers would be characterized as brittle, it is the microscopic viscous flow at the tip of the crack that makes the largest contribution to γ_p .

Table 1

Fracture Surface Energies at 25°C (12,13)

MATERIAL	γ_{calc} 10^3 ergs/cm^2	γ_{obs} 10^3 ergs/cm^2
Steel	1.0	1000
Glass	1.7	0.55
PMMA	0.5	200
Polystyrene	0.5	400

Examination of the fracture surfaces of glassy polymeric materials will yield valuable information concerning the mechanism of failure and the measured value of fracture surface work. The most important features of the fracture surface are the appearance of colors on the surface and the degree of roughness of the surface.

The appearance of colors supplies direct evidence for a viscous flow dissipative process as the crack propagates. The characteristics of the colors indicate that they are due to optical interference patterns in a thin layer at the fracture plane which arise as a result of an orientation effect of the polymers during fracture. This layer of material adjacent to the fracture plane is affected to a depth which approximates the wavelengths of visible light, and variations in layer thickness are reflected in differences in color. The presence of these interference colors in PMMA specimens tested at extremely low temperatures indicates that microscopic viscous flow occurs even at temperatures far below the glass transition.

For glassy polymers, the roughness of the fracture surface is a direct indication of the energy required for crack propagation. In addition, surface roughness also increases with crack velocity in tensile specimens. An examination of a typical fracture surface will reveal certain characteristic features which explains the fracture process and the relation of surface roughness to fracture energy (14, 15).

Near the origin of fracture a mirrorlike surface is generally observed, beyond which the fracture surface becomes more roughened (see Figure 2). At the initiating flaw, there is a great deal of energy absorption due to plastic deformation. From its origin, the fracture progresses slowly until it reaches its critical size for the applied stress, at which point it becomes unstable and propagates rapidly. The area of slow growth that contains the origin of fracture, known as the "mirror area", is smooth and of high specular reflectivity. This area is relatively featureless and only under high magnification is there some evidence of tear lines, indicating that relatively little energy is required for crack propagation in this area once the crack has started to grow.

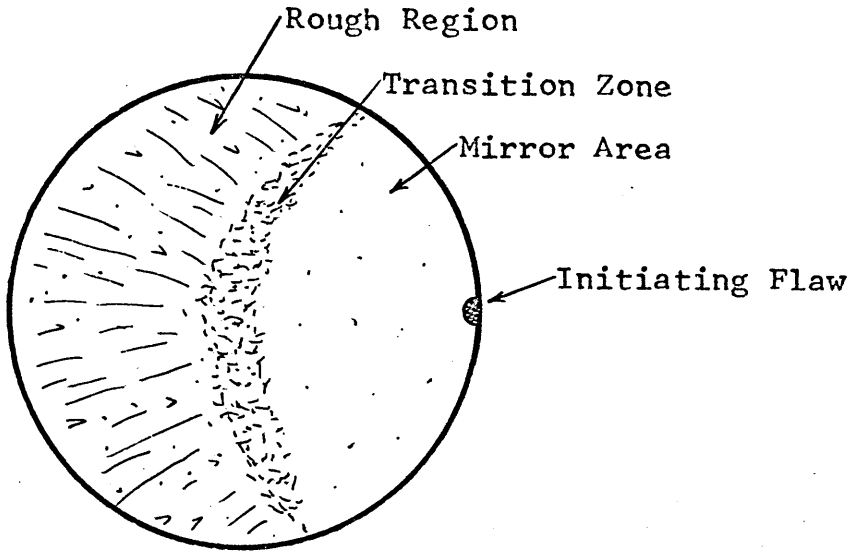

Figure 2 - Typical Fracture Surface (14)

The boundary between the mirror area and the rough region, referred to as the transition zone, is the line of demarkation between subcritical and critical crack growth. This region consists of irregular lines oriented in the direction of crack propagation. These lines mark the boundaries between fracture elements spreading forward on different levels and are called tear lines. Some irregularly shaped geometric figures may begin to appear in the transition zone due to slight advance nucleation of flaws caused by a higher stress level and crack velocity than in the mirror area. These markings suggest a higher toughness then in the mirror area.

Beyond the transition zone, large numbers of geometric figures resembling primarily parabolos and hyperbolos can be seen. By now, the stress field associated with the crack front is sufficiently high to initiate cracks at flaws ahead of the advancing crack front, leading to the onset of rapid growth as the multiplicity of cracks so created link up and generate the marked change in fracture surface appearance. The geometric figures are produced by the intersection of the main crack front with the secondary cracks propagating radially from the numerous local flaws as described above. The relative velocities of the two crack fronts determines the type of figure formed. Since the secondary fractures will generally not be coplanar with the main crack, tear

lines will develop where they link up. In this "rough region", still greater energy is required for crack propagation for the tear lines and the fracture origins represent the major deformation processes for which energy must be supplied for the fracture process.

Since the value of the fracture surface work, γ_p , is highly dependent upon microscopic phenomena, it would be expected that environmental conditions and changes in molecular structure would have a definite influence on the fracture behavior of polymeric materials. The effects of some of these variables have been determined (12, 13, 14, 15) and are described below. Note that the variables which affect the mechanical behavior of polymers also affect the appearance of the fracture surface.

Temperature - Results indicate that the fracture surface work increases as the temperature is reduced from +50°C to -200°C. A reduction in temperature tends to minimize the mirror or slow-growth area. The variation of γ_p of polystyrene and PMMA with temperature is shown in Figure 3. (Note the glass transition temperature of these polymers is approximately +100°C.)

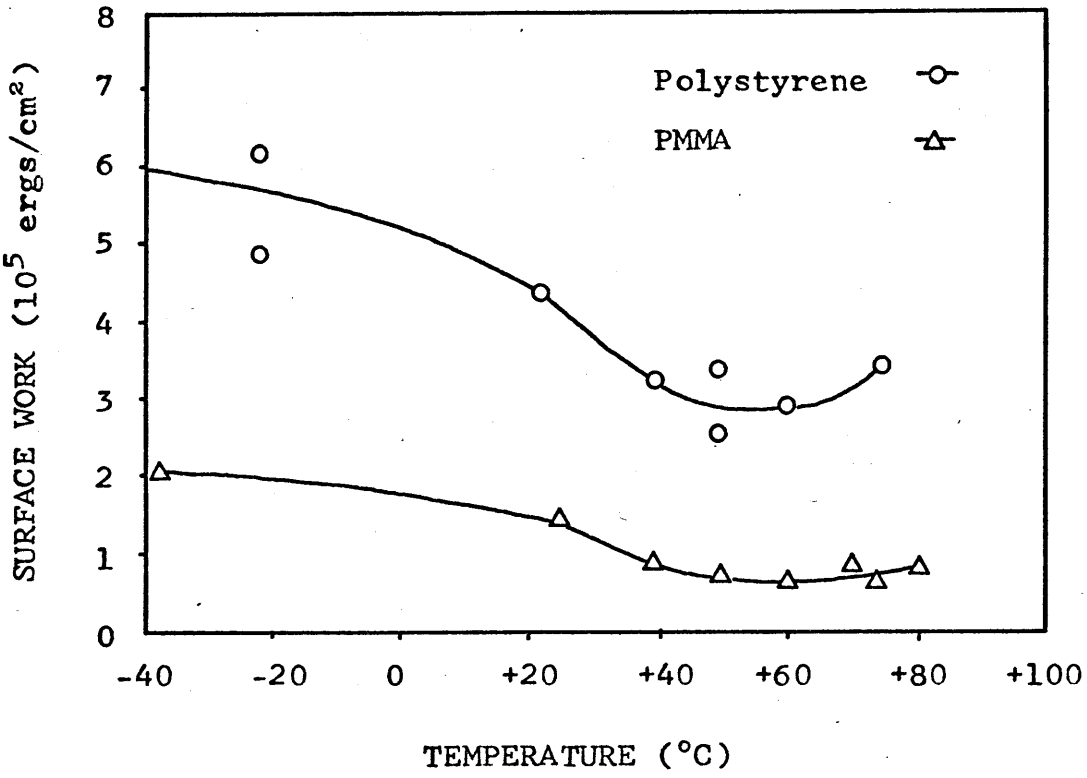

Figure 3 - γ_p versus Temperature (13)

Molecular Structure - Results for crosslinked polymers indicate that the surface work decreases as the degree of crosslinking increases. The surface work of a crosslinked polymer may be a factor of 10 less than that of a non-crosslinked (linear) polymer; however, γ_p of a crosslinked polymer is still 100 times greater than the theoretical value. The fracture surfaces of crosslinked polymers are usually less featured than those of non-crosslinked polymers, and the characteristic geometric figures and other easily distinguishable markings, such as those found in PMMA, are usually not observed, inferring less energy is required for fracture.

Molecular Weight - The surface work increases as the molecular weight, M_V, of a polymer increases (see Table 2). An increase in molecular weight tends to minimize the mirror area.

Table 2

Dependence of γ_p on Molecular Weight for PMMA (12)

$M_V \times 10^5$	γ_p, 10^5 ergs/cm^2
0.98	1.14
1.8	1.33
13.0	1.50
60.0	1.56

Molecular Orientation - The surface work decreases greatly as molecular preorientation is increased providing the crack is propagated parallel to the orientation. The fracture surfaces of PMMA preoriented specimens where the crack was propagated parallel to the orientation were mirror-smooth, and no interference colors were present which indicates that the thickness of the oriented film has either become very small or that no orientation is present. In other words, the crack could not produce as much molecular transport or orientation as usual, since the orientation of the polymer chains before the test was more nearly parallel to the direction of crack growth (13).

These effects due to the different variables can all be explained by considering the microscopic behavior which

occurs at the crack tip. As a general rule, higher surface work is usually associated with increased molecular transport (viscous flow) at the tip of the propagating crack. Increasing the temperature reduces the strength of the secondary van der Waal's bonding forces between molecules and allows them to flow easier. Consequently, increased temperature serves only to reduce the work necessary to orient the molecules, and hence, a lower surface work is measured at elevated temperatures. On the other hand, molecular crosslinks transform the linear chain structure into a three dimensional network which reduces the chain mobility and greatly limits viscous flow. Crosslinking imposes much higher energy barriers to molecular translational motion than does the reduction of internal molecular energy due to decreased temperatures and, thus, decreases plastic deformation at the tip of a propagating crack and reduces the fracture surface work. As for polymers with increased molecular weights, longer chain molecules require more work to orient them ahead of the growing crack. Finally, preoriented molecule chains parallel to the direction of crack growth need not undergo orientation during the fracture process and, therefore, decrease the fracture surface work.

Thus, brittle fracture theories have been applied to polymeric materials and much experimental data has been obtained for plexiglas and polystyrene. However, caution

must be taken in relating these findings to asphalt and asphaltic mixtures. Plexiglas and polystyrene are both pure polymers with known molecular structures and fairly constant molecular weights. Furthermore, these polymers were tested much below their glass transition temperatures which are in the range of +100°C. On the other hand, asphalt is not a pure polymer with a definite structure, but a multiphase polymer consisting of high molecular weight polymeric components dissolved or suspended in lower molecular weight polymers. Consequently, its molecular weight is not constant and varies greatly with respect to various conditions, such as degree of aging. In addition, the glass transition temperature of a polymer depends upon its chemical structure, including the size of molecular chain groups; i.e., its molecular weight (16). Tg also depends upon the composition of copolymers according to a weighted average of the glass temperatures of its component homopolymers (16). Thus, the glass transition temperatures of asphalts are not only orders of magnitude lower than the Tg's of plexiglas and polystyrene (17), but they tend to vary as much as molecular weight varies. Therefore, asphalt is an extremely complex polymeric material, and its brittle fracture behavior may not be as well defined as that of the polymeric materials which have already

been discussed.

Determination of the Critical Strain-Energy Release Rate

The modified Griffith theory of brittle fracture has been applied to asphalts (3) which were subjected to different conditions of temperature, rate of loading, and degree of aging. At sufficiently low temperatures, the asphalts tested did behave as brittle, amorphous materials, and the critical strain-energy release rate was calculated. As would be expected, the value of the critical strain-energy release was influenced by the rate of loading, the test temperature, the type of asphalt, and the degree of aging.

The critical strain-energy release rate, G_c, was determined by the analytical method, as discussed by Kaplan (18). This method employs the testing of a notched beam in bending. Since this type of test employs a surface notch, the expression for strain-energy release rate, Equation 7, must be divided by two due to the fact that there is only one point of stress concentration. Furthermore, since the dimensions of the test specimen are such that a state of plain strain exists, E must be replaced by $E/(1-\nu^2)$. These modifications give

$$G = \frac{\pi(1-\nu^2)c\sigma^2}{E} \qquad \text{Equation 10}$$

as the expression for strain-energy release rate. For the case of rectangular beams, Winnie and Wundt (19) have shown that Equation 10 may be written in the form

$$G = \frac{(1-\nu^2)\sigma_n^2 h}{E} f(c/d) \qquad \text{Equation 11}$$

where σ_n is the nominal bending stress at the root of the notch, f(c/d) is a function of the notch depth ratio, and h is the net depth of the beam at the notch. Since the test is run by increasing the load applied to the test specimen until a stress level is reached which results in rapid propagation of the initial crack, Equation 11 becomes the expression for Gc, the critical strain-energy release rate.

The analytical method of determining G_c will be used in this continued study of fracture in asphalt and asphaltic mixtures. Marsh (3) determined that the value of G_c is independent of the size of the notch in the asphalt specimens; therefore, only one notch size need be used in determining the charactistic G_c value for the asphalt specimens subjected to various conditions. This study will extend the investigation of asphalt fracture to cover the effects of wider ranges of temperature variation and the effects of varying amounts of mineral filler to form asphaltic mixtures on the fracture behavior of asphalt.

OBJECTIVES AND SCOPE

The objective of this study is to apply the Griffith theory of brittle fracture to the fracture of asphalt and asphaltic mixtures in order to gain additional knowledge of the fracture phenomena of asphalt and to determine possible means of improving the fracture toughness of asphalt at low temperatures. To accomplish this objective, two asphalts with different rheological properties were mixed with various percentages of mineral filler and tested under different thermal conditions. In addition, the effect of aging the asphalts was investigated, and the effect of using a different testing procedure was examined. The variables included five test temperatures, four percentages of filler additive, and two degrees of aging, as given in Table 3. Each type of asphalt was tested at a minimum of three temperatures for each variation in mineral filler content and degree of aging, with at least one temperature above and below their respective glass transition temperatures.

Table 3

Test Variables Used in this Study

TEMPERATURE	B-3056	-20°F	-10°F	0°F	+10°F
	B-2960	-30°F	-20°F	-10°F	0°F
% of MINERAL FILLER by WEIGHT of ASPHALT		0%	25%	50%	75%
AGING at 375°F		0 HOURS		6 HOURS	

MATERIALS

The two asphalts used in this study were an AC-20 grade asphalt cement coded B-3056 produced by the American Oil Company and an AC-20 grade asphalt cement coded B-2960 produced by the Shell Oil Company. Both of these asphalts were used in the "Asphalt Institute - Bureau of Public Roads Cooperative Study of Viscosity-Graded Asphalts". The results of conventional tests on the asphalts are shown in Table 4.

A plot of data showing shear rate versus shear stress for the two asphalts at a test temperature of 25°C is given in Figure 4. This log-log presentation results in a straight line and can be represented by

$$\tau = A(\dot{\gamma})^{n} \qquad \text{Equation 12}$$

where A and n are constants which vary with the test temperature. The slope of the lines in Figure 4 is the inverse of n and would be unity for a perfectly Newtonian material. As n deviates from unity, the behavior of the material becomes more non-Newtonian. Therefore, the relative Newtonian response of the two asphalts can be determined from this plot, and it is seen that the B-2960 asphalt is more Newtonian than the B-3056 asphalt. Moavenzadeh and Stander (20) point out that the value of n decreases with decreasing temperature, thus indicating a more non-Newtonian response at lower temperatures. They further indicated that, for both asphalts, the pseudo-plastic behavior increases with decreasing temper-

ature and increases with increased aging.

The mineral filler used in this study was flint powder. All of the fine grained silica particles passed through the #200 sieve.

Table 4

Results of Typical Tests on Asphalts Used in this Study (20)

TEST	ASPHALT	
	B-3056	B-2960
Specific Gravity	1.020	1.034
Softening Point, Ring and Ball	— — —	125°F
Ductility 77°F	250+cm	— — —
Penetration 200gm, 60 sec, 39.4°F	30	— — —
Flash Point, Cleveland Open Cup	545°F	515°F
Glass Transition Temperature *	-1.3°F	-20.2°F
Viscosity at 140°F, poises x 10^2 *	26.8	20.6

* Reference 17

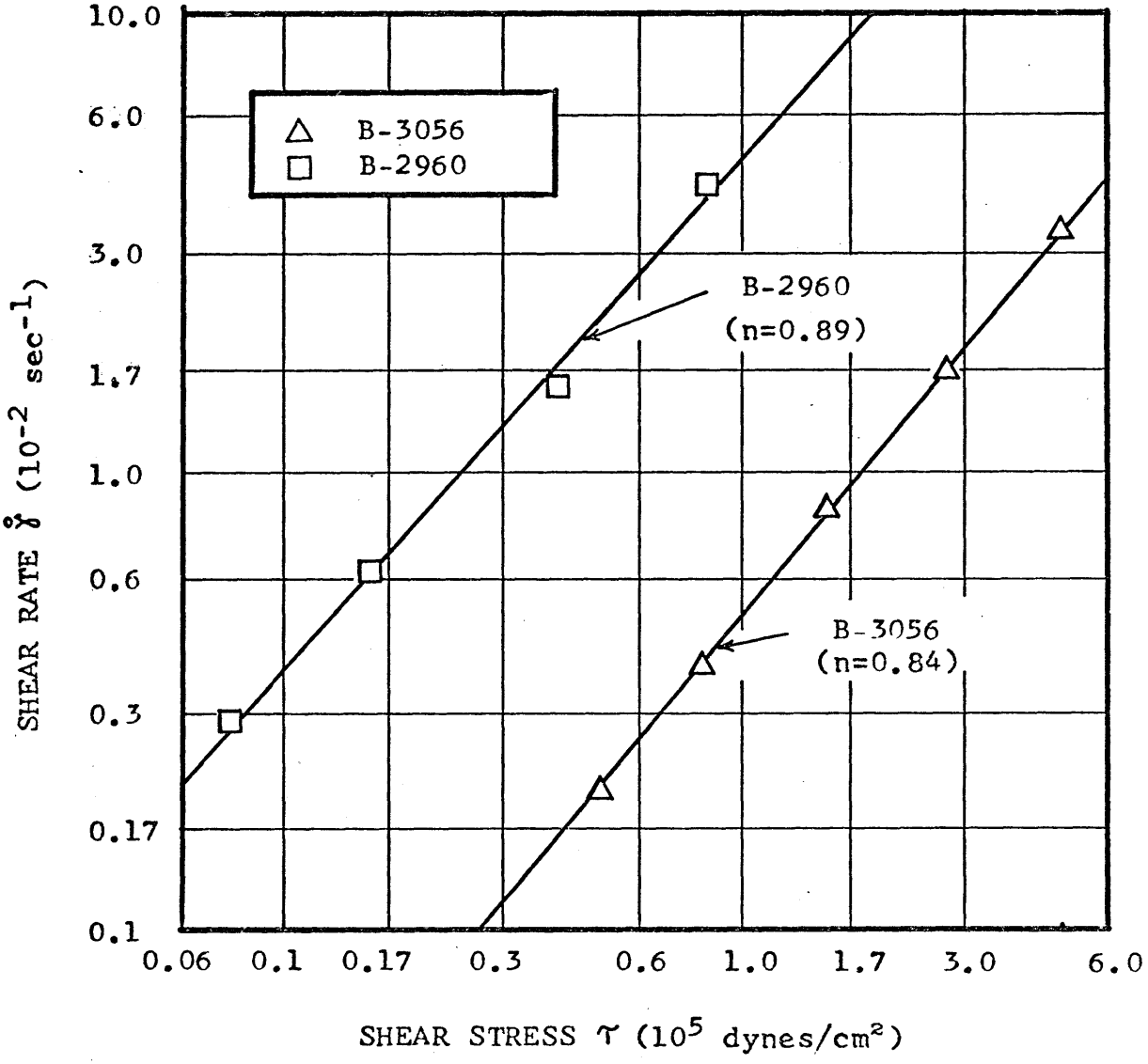

Figure 4 - Shear Rate versus Shear Stress at 25°C (20)

PROCEDURE

Specimen Preparation

The specimens used in this study were five-inch long asphalt beams with a cross section measuring one-half inch by one-half inch. Half of the specimens tested were unnotched; the other half contained a three-sixteenths of an inch notch at midspan. The notch geometry and the three point bending method of loading are shown in Figure 5. The notches were formed by an insert in the mold.

To make the specimens, the asphalt was heated to 135°C for one hour so that it would be fluid enough to pour into a similarly heated mold. The mold was overfilled slightly to allow for a decrease in volume as the asphalt cooled. The heated mold kept the asphalt fluid enough to allow any entrapped air to float to the surface in the form of bubbles. After cooling to room temperature, the mold was placed in a refrigerator and cooled until the asphalt hardened. Before the beams were removed from the mold, the excess asphalt was removed using a warm spatula. A coating of high vacuum grease on the molds prevented the asphalt from adhering to the steel and greatly facilitated the removal of the beams from the molds. The prepared beams were stored in a freezer at -20°C until tested. The beams were placed either in a plexiglass box or under aluminum foil to protect them from moisture during storage.

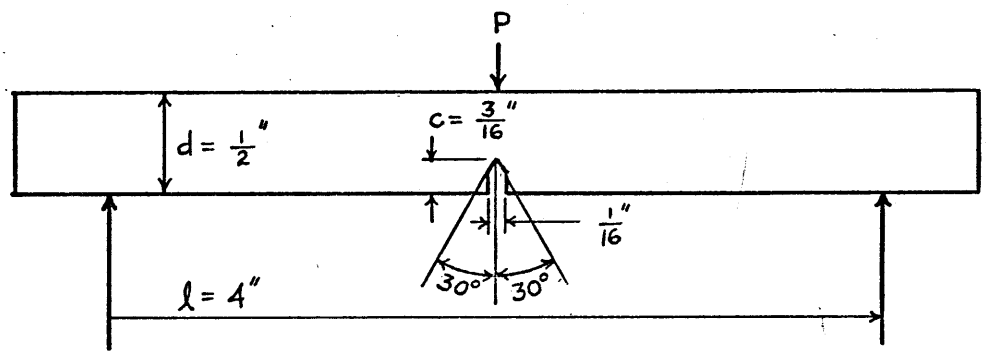

Figure 5 - Notch Geometry and Method of Loading

The beams containing mineral filler were prepared in essentially the same way. When the heated asphalt was removed from the oven, the proper amount was poured into a heated mixing bowl containing flint powder so that the desired percentage of mix was obtained. The flint powder was preheated to 135°C to remove any moisture and to allow thorough mixing with the asphalt. The filler and asphalt were blended together for two minutes in a mechanical mixer. The mixture was then poured into a heated mold and the remainder of the specimen preparation process was the same as described above.

Aging of the Asphalt

Aging of the asphalts was accomplished by heating the asphalt to 135°C for one hour, then pouring it onto a shallow eleven-inch by nineteen-inch enameled steel tray. This formed a film of asphalt approximately one-eighth of an inch deep across the entire tray which was then heated in an oven at 375°F (190°C) for six hours. The aged asphalt

was then poured into heated molds and the beam preparation process was followed.

Testing

The bending tests were run on an Instron Testing Machine. The tests were performed in an air-circulating chamber which was placed directly in the testing machine. Initially, a silicone oil constant temperature bath was used to provide the thermal environment for the test specimens. Liquid nitrogen was dripped into a pan beneath the plexiglas box containing the silicone oil to maintain the oil at the low test temperatures. The specimens were kept at the test temperature at least 20 minutes before testing, and the specimens were tested submerged in the oil. (See Figure 6).

However, figuring that the silicone oil affected the test results, especially those for the notched beams, the silicone oil bath was discarded and circulating air chilled by evaporating liquid nitrogen was used to obtain the test temperature. The temperature was controlled manually by adjusting the flow of liquid nitrogen into the chamber. The temperature was controlled to ±1.0°C. Again the specimens were kept at test temperature at least 20 minutes before testing. Testing in the atmosphere also allowed visual observation of the specimen, which proved to be a significant

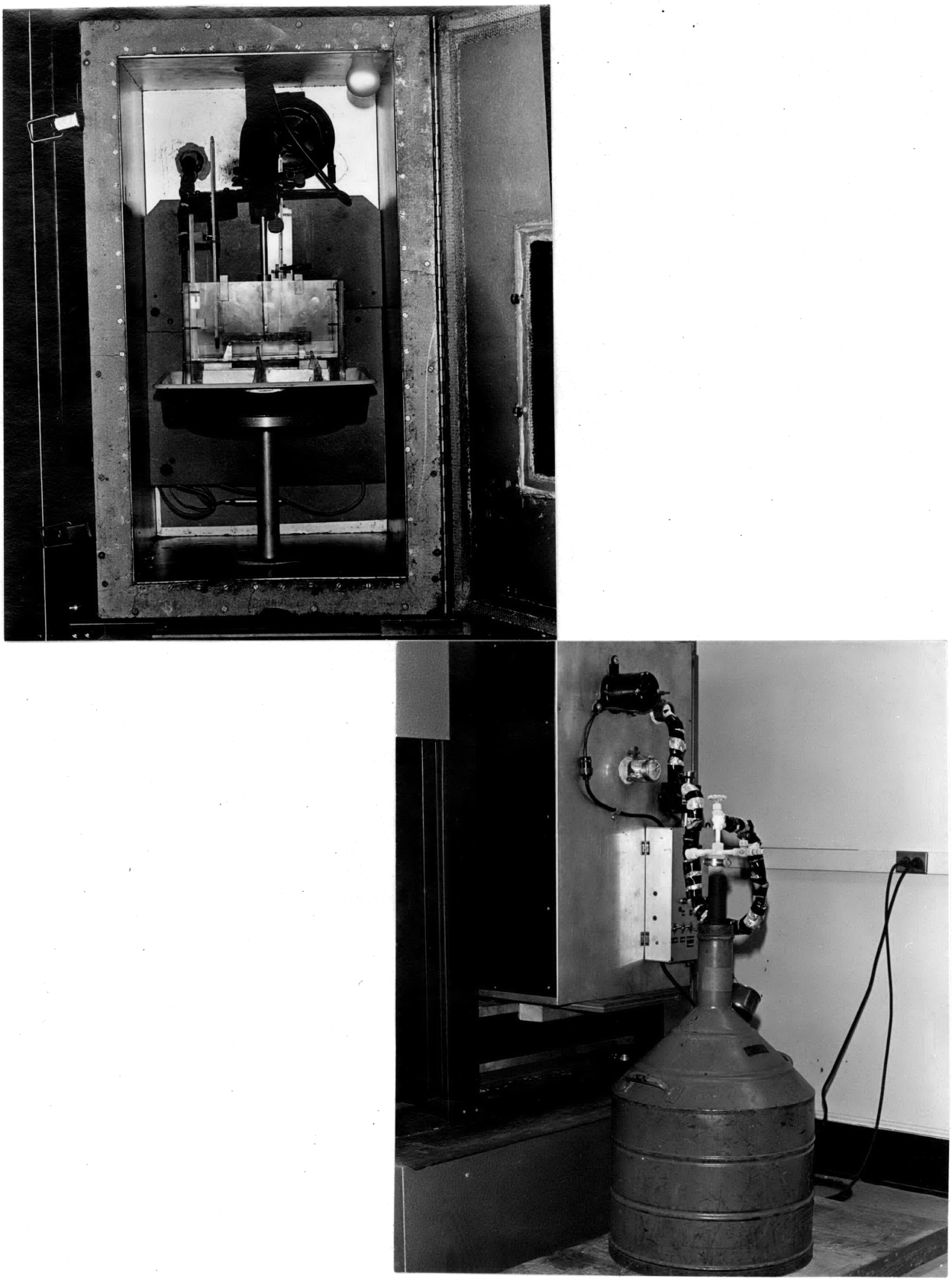

Figure 6 - Apparatus for Testing Beams in Silicone Oil

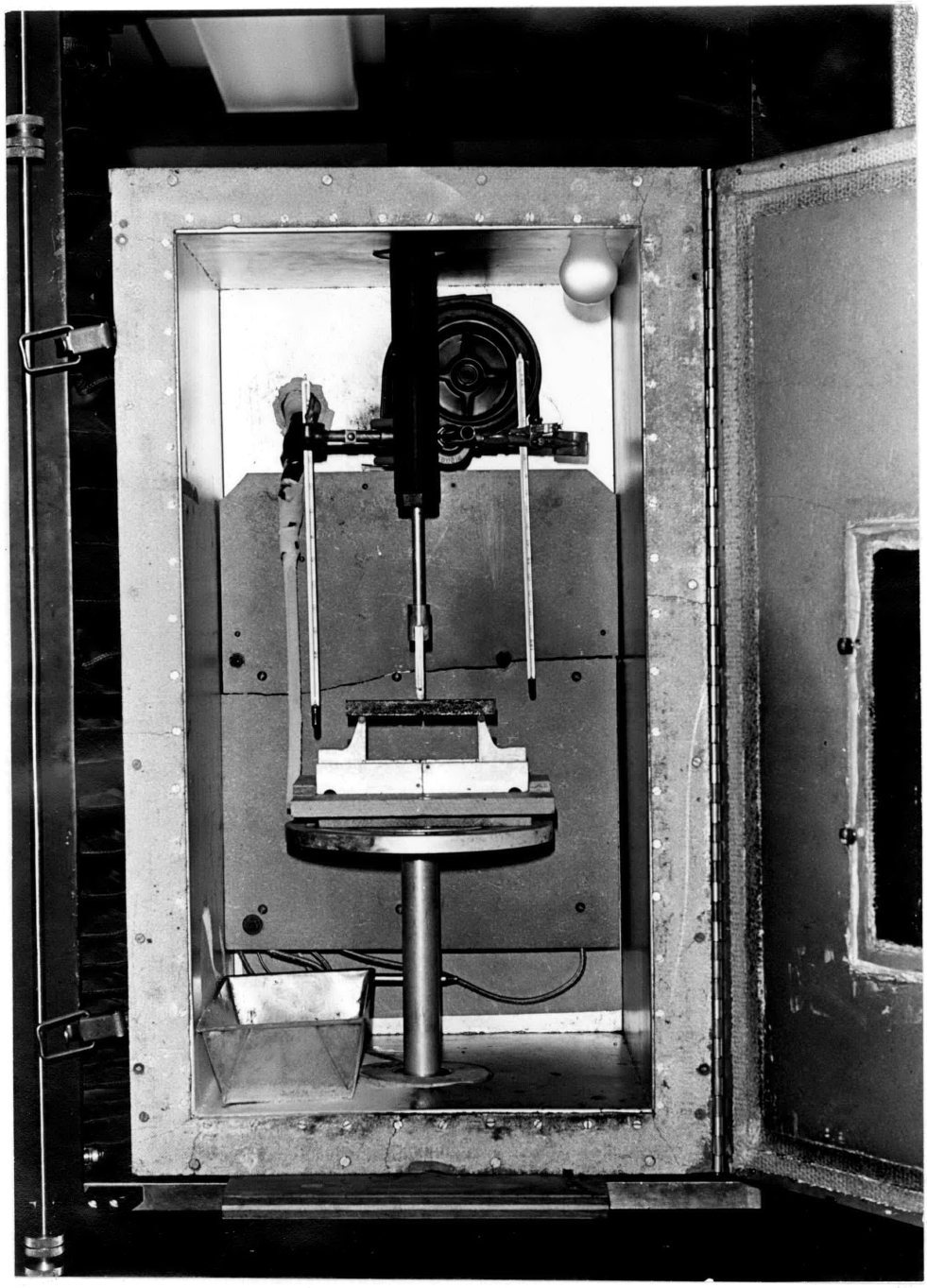

Figure 7 - Apparatus for Testing Beams in the Atmosphere

advantage over testing in the silicone oil bath. (See Figure 7).

A constant loading rate of 0.10 inches per minute was used for most tests. Data output consisted of a plot of load versus time. A minimum of six beams (three notched and three unnotched) was tested for each combination of test temperature and type of specimen.

Calculation of E and G_c

In all tests, the load increased continuously with a constant rate until the specimen failed in a catastrophic manner. A schematic diagram of the load-deflection curve is shown in Figure 8.

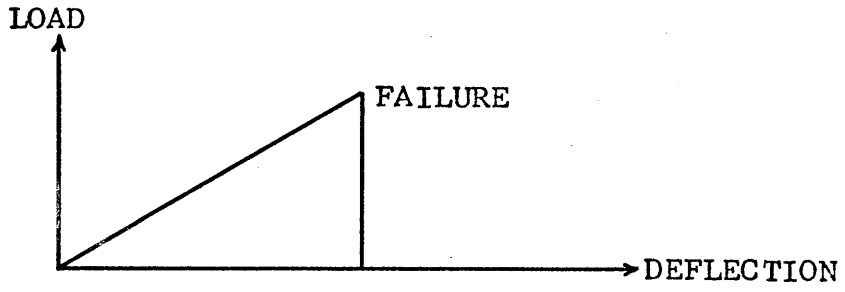

Figure 8 - Schematic Load-Deflection Diagram

The modulus of elasticity, E, for each set of test conditions was determined using the slopes of the load-deflection curves for unnotched beams and the standard deflection formula for a three point bending test, which is

$$Y = \frac{1}{48} \cdot \frac{P\ell^3}{EI} \qquad \text{Equation 13}$$

where Y is the maximum deflection of the beam, ℓ is the span length, P is the applied load, and I is the moment of inertia of the beam. For the specimen geometry used in this study

$$E = 256 \cdot \frac{P}{Y} \text{ (PSI)} \qquad \text{Equation 14}$$

where P/Y is the slope of the load-deflection curve for an unnotched beam. The average modulus of elasticity of at least three tests was calculated for each test condition.

The critical strain-energy release rate, G_c, was determined using the maximum loads required to break the notched specimens and Equation 11, which is rewritten here for convenience.

$$G_c = \frac{(1-\nu^2)\,\sigma_n^2\, h}{E} f(c/d) \qquad \text{Equation 11}$$

The value of E was determined as described above and Poisson's ratio, ν, was assumed to be one-half in all cases. The value of σ_n, the nominal bending stress at the root of the notch, was determined using the standard flexure formula

$$\sigma_n = \frac{M_b c_n}{I_n} \qquad \text{Equation 15}$$

where M_b is the bending moment at the notched section of the beam, C_n is one-half the depth of the unnotched portion of the beam at the notched cross section, and I_n is the moment of inertia of the notched cross section. For the notch depth ratio of the beams used in this study, f(c/d) is equal

to 0.47 (18). Considering the geometry of the notched specimens, Equation 11 becomes

$$G_c = 1665 \cdot \frac{P_{max}^2}{E} \left(\frac{\text{IN-lb}}{\text{IN}^2}\right) \qquad \text{Equation 16}$$

where P_{max} is the load required to break the notched specimens. Again, a minimum of three tests were run to calculate G_c for each test condition. The values of E, P_{max}, and G_c were converted to metric units using the appropriate conversion factors.

RESULTS AND DISCUSSION OF RESULTS

The results of the mid-span bending tests on the asphalt beams are presented and discussed in this section. The values of the modulus of elasticity, E, the load required to fracture the notched specimens, P_{max}, and the critical strain-energy release rate, G_c, for all the combinations of test conditions are presented in the included tables. The effects of the different test variables are presented in the form of graphs and are discussed under the following topics: effect of temperature, effect of different asphalts, effect of mineral filler, effect of aging, effect of testing in oil, and effect of rate of loading.

Effect of Temperature

The values of E, P_{max}, and G_c for both asphalts tested at various temperatures are presented in Table 5 and are plotted in Figures 9 and 11. For the range of test temperatures, the modulus of elasticity increases for both asphalts as the temperature decreases. This is the expected behavior for asphalt since it is a thermoplastic material. The marked increase in E in the glass transition region is especially noticeable for B-3056 asphalt.

The maximum load required to break the notched beams also increases as the temperature decreases. However, for the range of test temperatures used in this study, E increases

at a much greater rate than P_{max}, and since G_c calculated by the analytical method is proportional to P_{max}^2/E, the value of G_c for both asphalts decreases as the temperature decreases.

A possible explanation of this behavior can be inferred from the physical-chemical structure of asphalt. The structure of asphalt is generally described as a three phase colloidal system consisting of asphaltenes, resins, and oils (21). The asphaltenes are the highest molecular weight materials in asphalt and are primarily of an aromatic nature with very few side chains attached. The resins are the intermediate molecular weight materials, and they contain more side chains than the asphaltenes. The oils are the lightest molecular weight materials in the asphalt and generally have a large number of chains in proportion to the number of rings. At low temperatures, the asphaltenes are precipitated from the oil-resin solution and exist as relatively associated complexes. The asphaltene molecules become practically immobile and trap the oily constituents by strong association bonds which are formed throughout the structure. The agglomeration of asphaltenes causes the asphalt to become more viscous and more brittle. This agglomeration tends to decrease the amount of molecular transport, or microscopic plastic flow, ahead of the crack and thus decreases the value of G_c. As the temperature increases, still remaining in the low temperature region around the glass transition temperature, dissociation of the large asphaltene molecules occurs and

microscopic viscous flow becomes more likely. The smaller oily molecules still remain trapped in the asphaltenes though, for if they were released into the system, macroscopic viscous flow would occur and the asphalt would no longer behave elastically.

The decrease in G_c with decreasing temperature for the asphalts in this study is contrary to the general behavior of the other glassy polymers previously discussed. The fracture surface work of polystyrene and PMMA increases as the temperature decreases. However, most of the testing of polystyrene and PMMA was done at temperatures far below their glass transition temperatures, and as can be seen in Figure 3, the fracture surface work of polystyrene starts to increase with increasing temperature at temperatures approaching the glass transition. Since the test temperatures used in this on asphalt are closely grouped around the respective glass transition temperatures of the two asphalts, it seems reasonable that G_c should increase with increasing temperature over this temperature range.

It should be noted that above 0°F for B-2960 asphalt, significant macroscopic inelastic responce of the specimens is observed which invalidates the theory used to determine the values of G_c.

Table 5 - Data Summary for Unaged Asphalts with 0% Filler ($\dot{\delta}$ =.10in/min)

ASPHALT		TEMPERATURE				
		-30°F	-20°F	-10°F	0°F	+10°F
B-2960	E 10^7 dynes/cm²	550	409	277	182	
	P_{max} 10^5 dynes	7.46	6.84	6.26	5.81	
	G_c 10^4 ergs/cm²	1.033	1.164	1.441	2.060	
B-3056	E 10^7 dynes/cm²		935	628	481	306
	P_{max} 10^5 dynes		5.82	5.35	5.15	4.53
	G_c 10^4 ergs/cm²		0.368	0.465	0.564	0.680

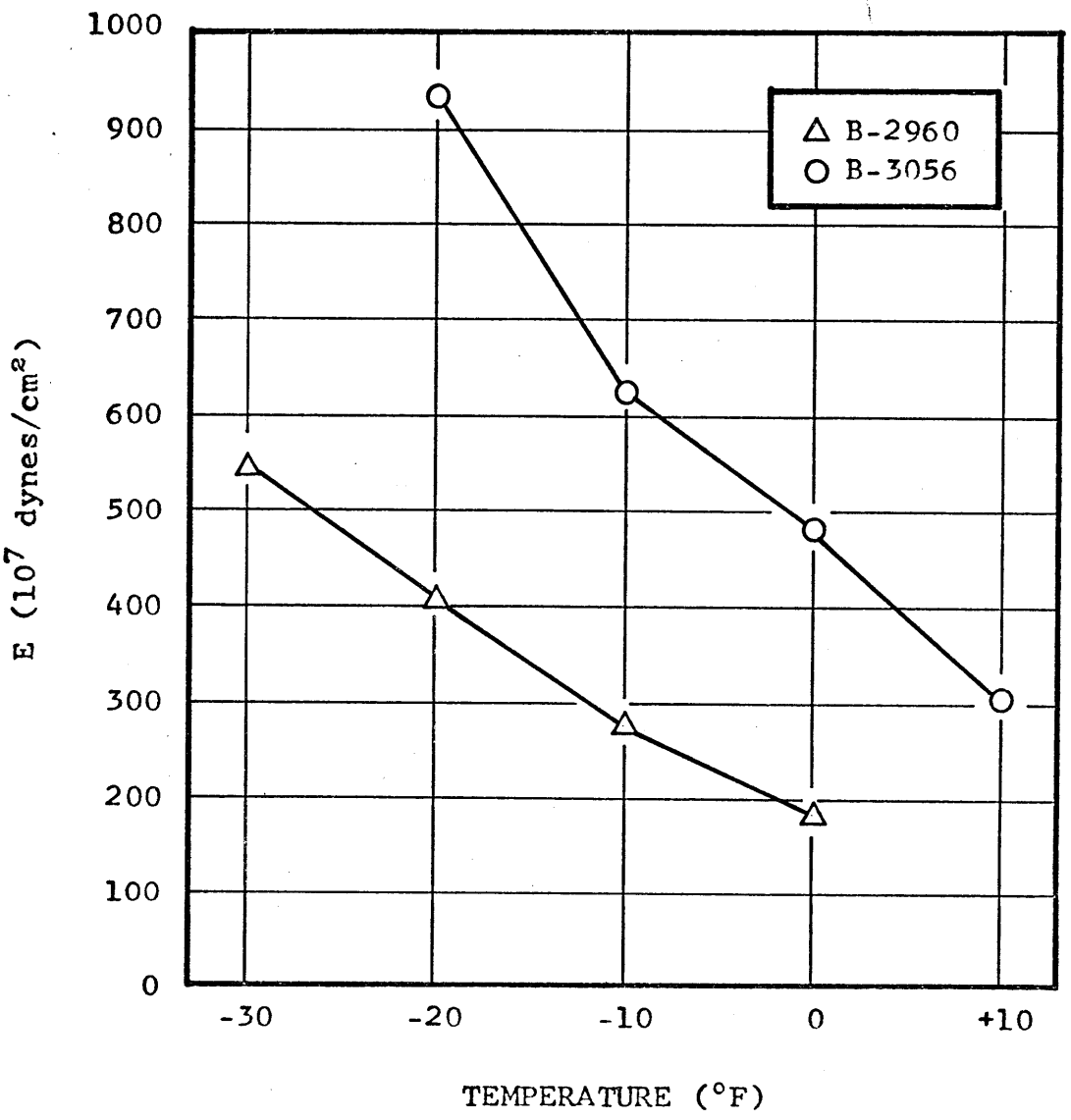

Figure 9 - E versus Temperature for B-2960 and B-3056 Asphalt Loaded at .10 in/min

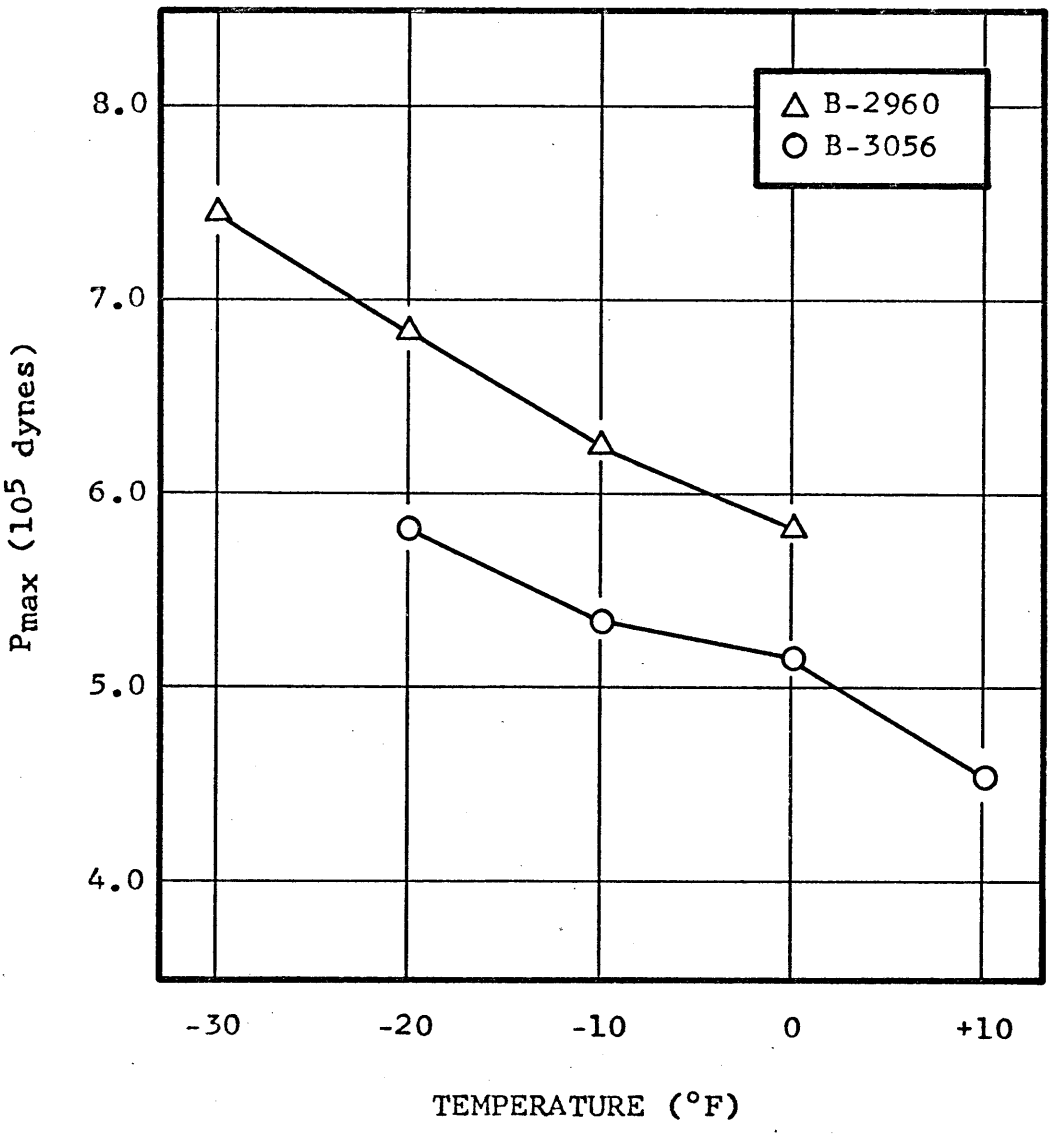

Figure 10 - P_{max} versus Temperature for B-2960 and B-3056 Asphalt Loaded at .10 in/min

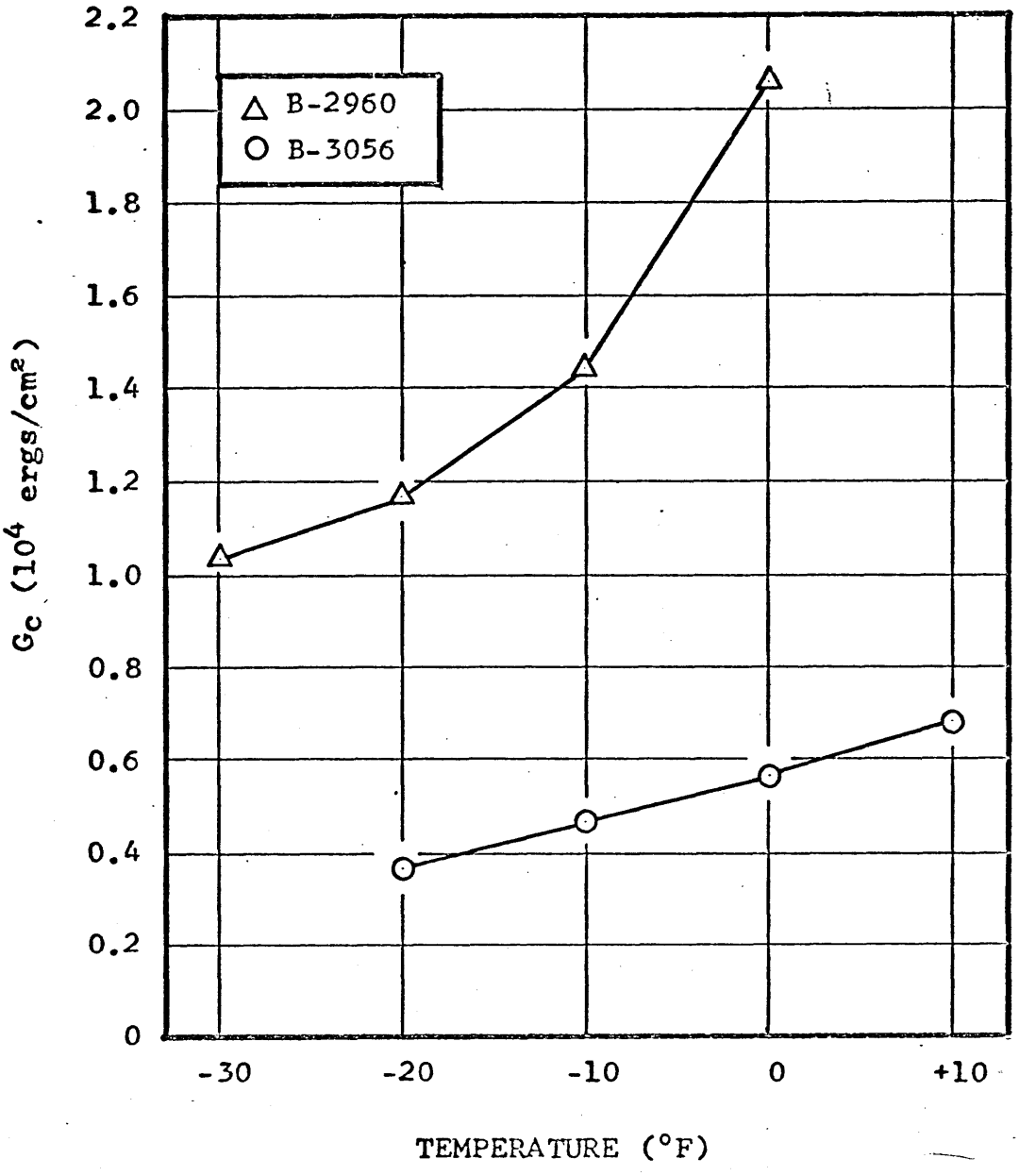

Figure 11 - G_c versus Temperature for B-2960 and B-3056 Asphalt Loaded at .10 in/min

Effect of Different Asphalts

Figures 9 through 11 are also used to compare the two asphalts used in this study. The plot of G_c versus temperature in Figure 11 reveals that the values of G_c for B-2960 asphalt are approximately three times greater than the corresponding values of G_c for B-3056 asphalt. Furthermore, B-2960 asphalt appears to be more temperature sensitive than B-3056 over the range of test temperatures used. This behavior can be explained by the fact that B-3056 asphalt is more non-Newtonian than B-2960 asphalt. Non-Newtonian behavior is a function of the degree to which the asphaltenes can be taken into solution by the oils. The asphaltenes in B-3056 are poorly integrated; whereas, those in B-2960 are well integrated (20).

Comparing the two asphalts used in this study with other materials, see Table 1, it can be seen that the fracture surface work ($\gamma_p = 1/2\ G_c$) for these asphalts is approximately an order of magnitude greater than that of inorganic glass, and approximately an order of magnitude less than that of plexiglas (PMMA). This seems reasonable since it has been shown that fracture surface work is a function of the molecular weight of a polymer. The molecular weight of PMMA is approximately 100 times greater than that of asphalt.

Even though the asphalts tested are polymers with molecular weights far less than PMMA, their measured values of fracture surface work are still nearly twenty times greater than the

theoretical value for glassy polymers. This indicates that microscopic inelastic flow processes must be occurring at the tip of the propagating crack in the asphalt.

Effect of Mineral Filler

The values of E, P_{max}, and G_c for both types of asphalt mixed with mineral filler are given in Table 6. In Figures 12 and 13, the values of G_c are plotted versus percentage of filler by weight of asphalt for B-2960 and B-3056 asphalt, respectively. For both asphalts, it can be seen that the value of G_c is increased between 2 1/2 and 3 times as the percentage of filler is increased from 0% to 75%. For each type of asphalt, the absolute increase in G_c for an increase in filler content from 0% to 75% is nearly the same at each test temperature: being approximately 1.6×10^4 ergs/cm^2 for B-2960 asphalt and 0.8×10^4 ergs/cm^2 for B-3056 asphalt.

G_c is plotted versus temperature for various percentages of filler mixed with B-2960 and B-3056 asphalt in Figures 14 and 15, respectively. From these plots it can be seen that the greatest increase in G_c occurs between 50% and 75% filler. This marked increase is especially evident at or below the glass transition temperatures of the respective asphalts.

The reason for the increase in fracture toughness as the filler content is increased becomes apparent on examining the fracture surfaces of the asphalt beams containing mineral filler. The fracture surfaces of these beams are very rough

Table 6 - Data Summary for Asphalts with Mineral Filler ($\dot{\delta}$ =.10 in/min)

ASPHALT	TEMP	% FILLER	E 10^7 dynes per cm^2	P_{max} 10^5 dynes	G_c 10^4 ergs per cm^2
B-2960	-10°F	0	277	6.26	1.441
		25	336	8.53	2.210
		50	486	11.30	2.680
		75	549	12.80	3.071
	-20°F	0	409	6.84	1.164
		25	492	8.88	1.630
		50	612	10.61	1.872
		75	815	14.92	2.781
	-30°F	0	550	7.46	1.033
		25	645	8.70	1.198
		50	838	11.76	1.679
		75	948	15.60	2.607
B-3056	0°F	0	481	5.15	0.564
		25	516	6.17	0.756
		50	592	7.37	0.936
		75	675	9.95	1.498
	-10°F	0	628	5.35	0.465
		25	823	6.75	0.565
		50	866	7.64	0.686
		75	1154	12.09	1.290
	-20°F	0	935	5.82	0.368
		25	870	6.35	0.474
		50	1201	8.84	0.662
		75	1271	12.13	1.179

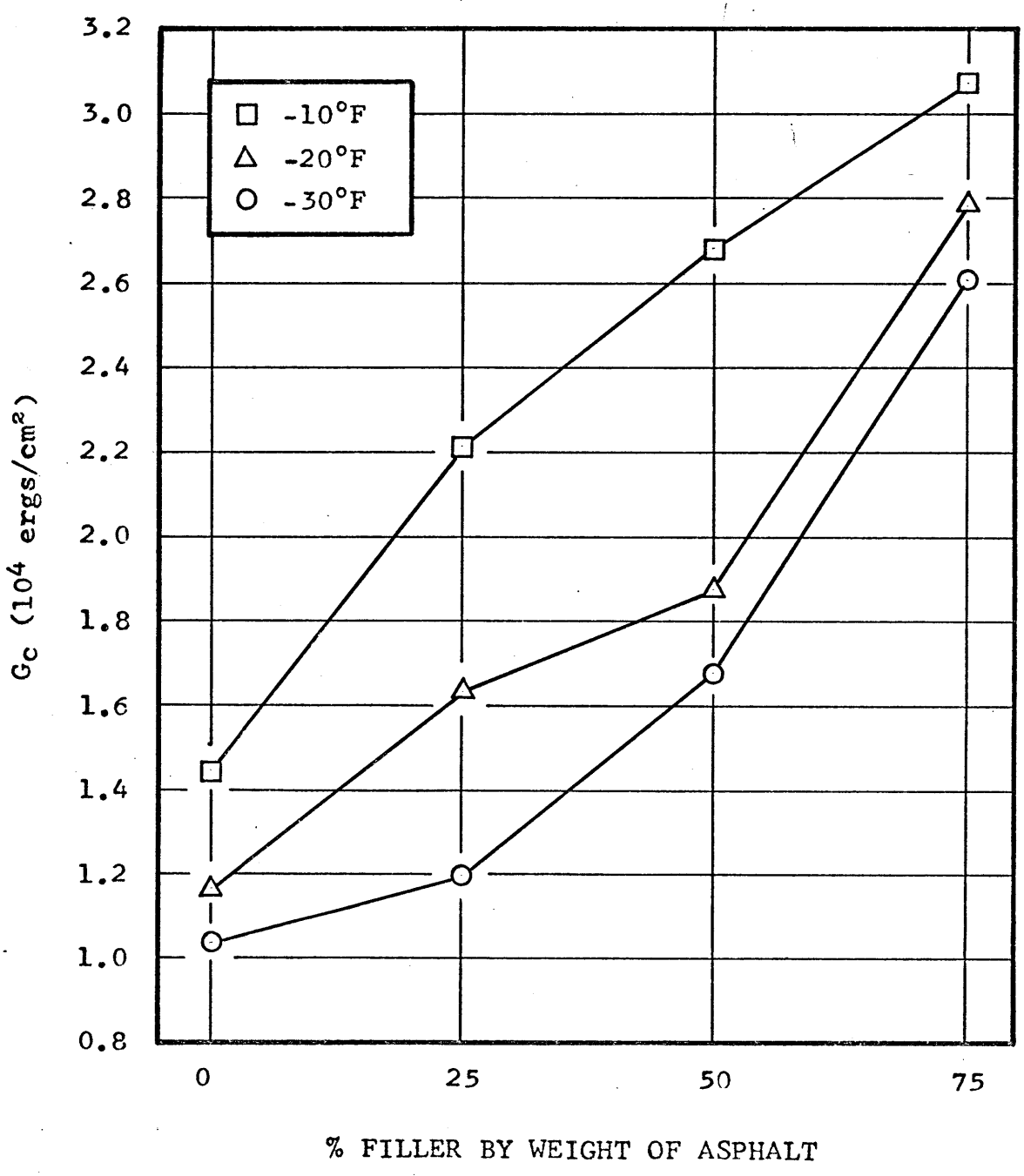

Figure 12 - G_c versus % Filler for B-2960 Asphalt Loaded at .10 in/min

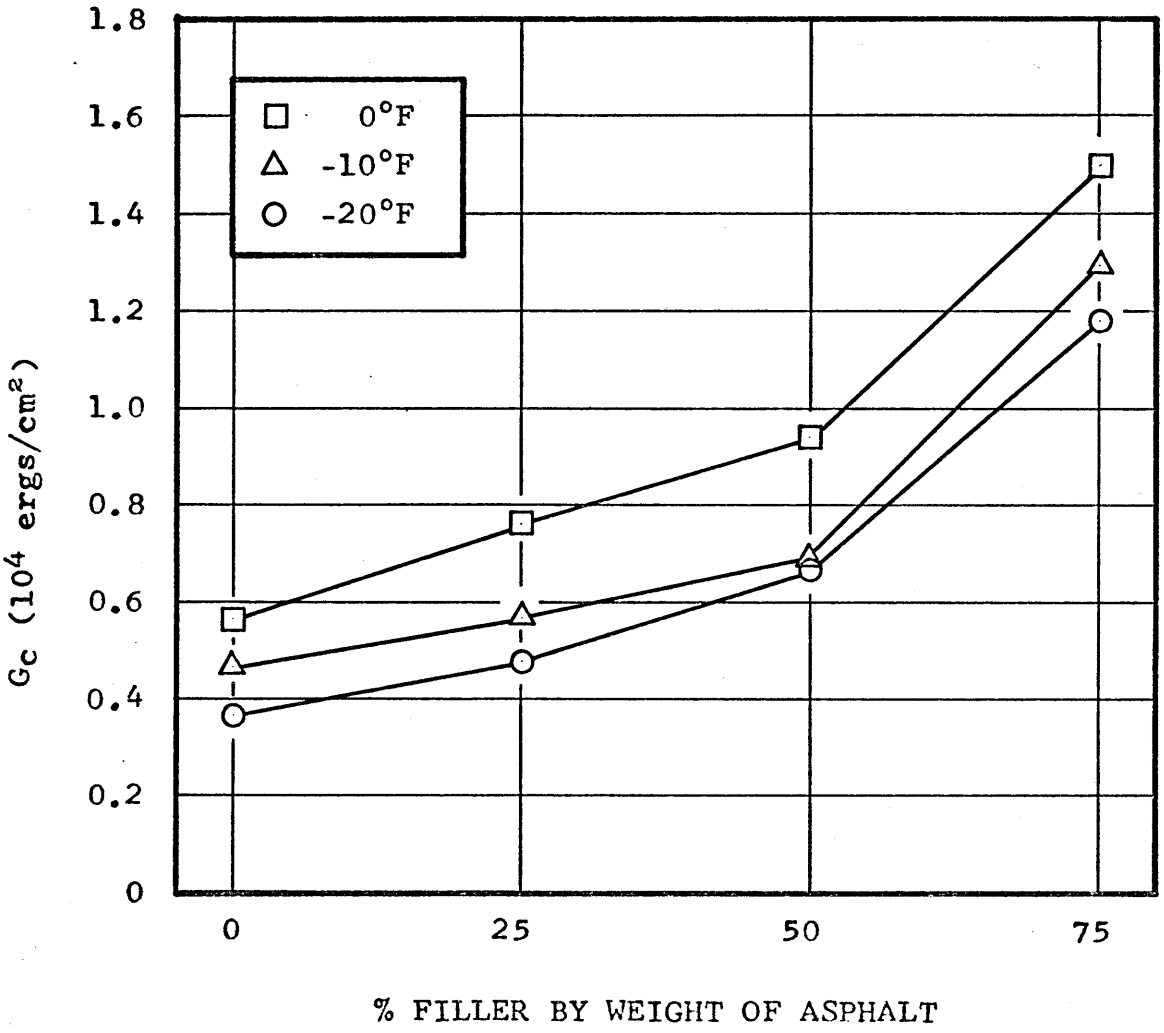

Figure 13 - G_c versus % Filler for B-3056 Asphalt Loaded at .10 in/min

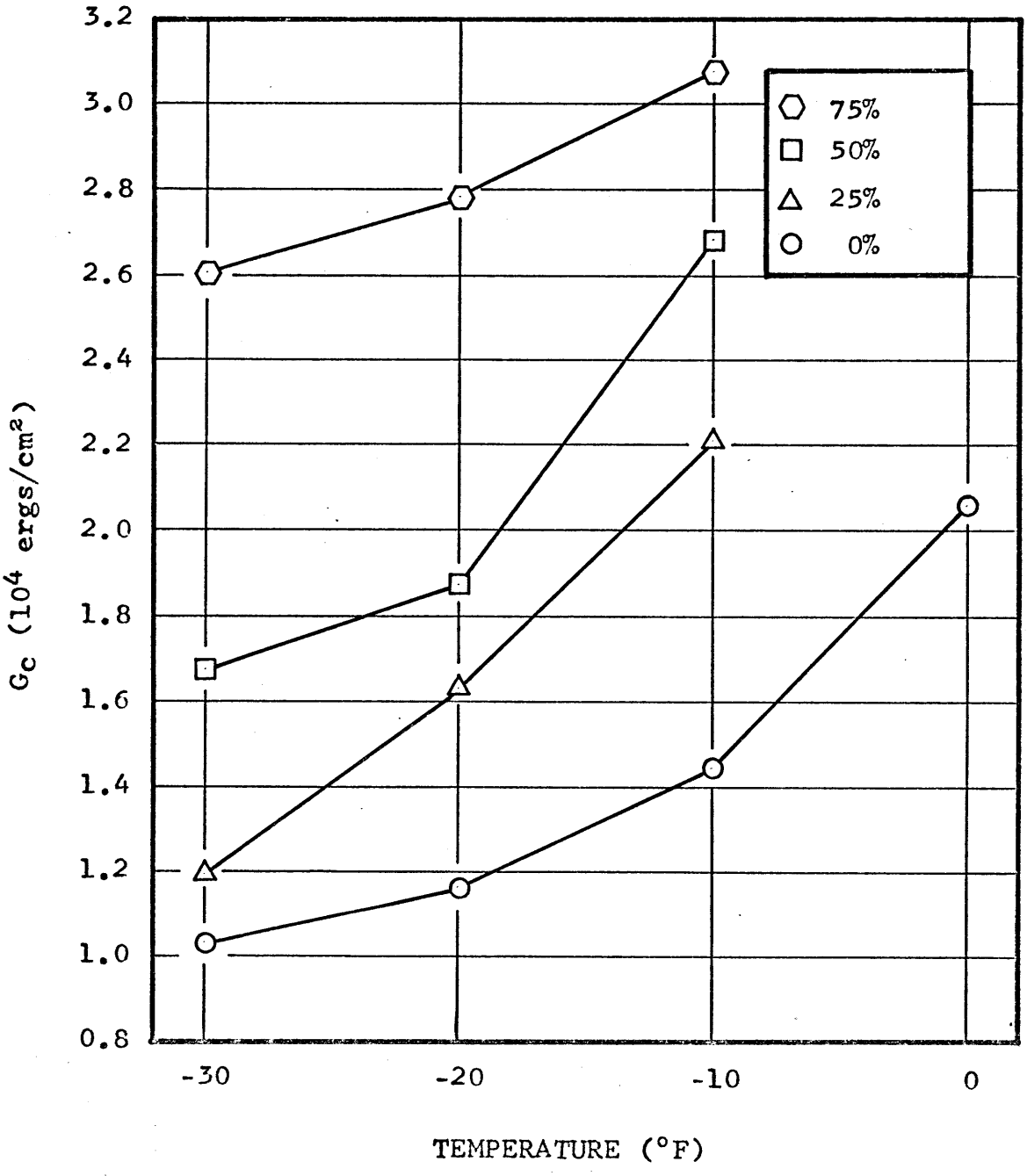

Figure 14 - G_c versus Temperature for B-2960 Asphalt mixed with Filler and Loaded at .10 in/min

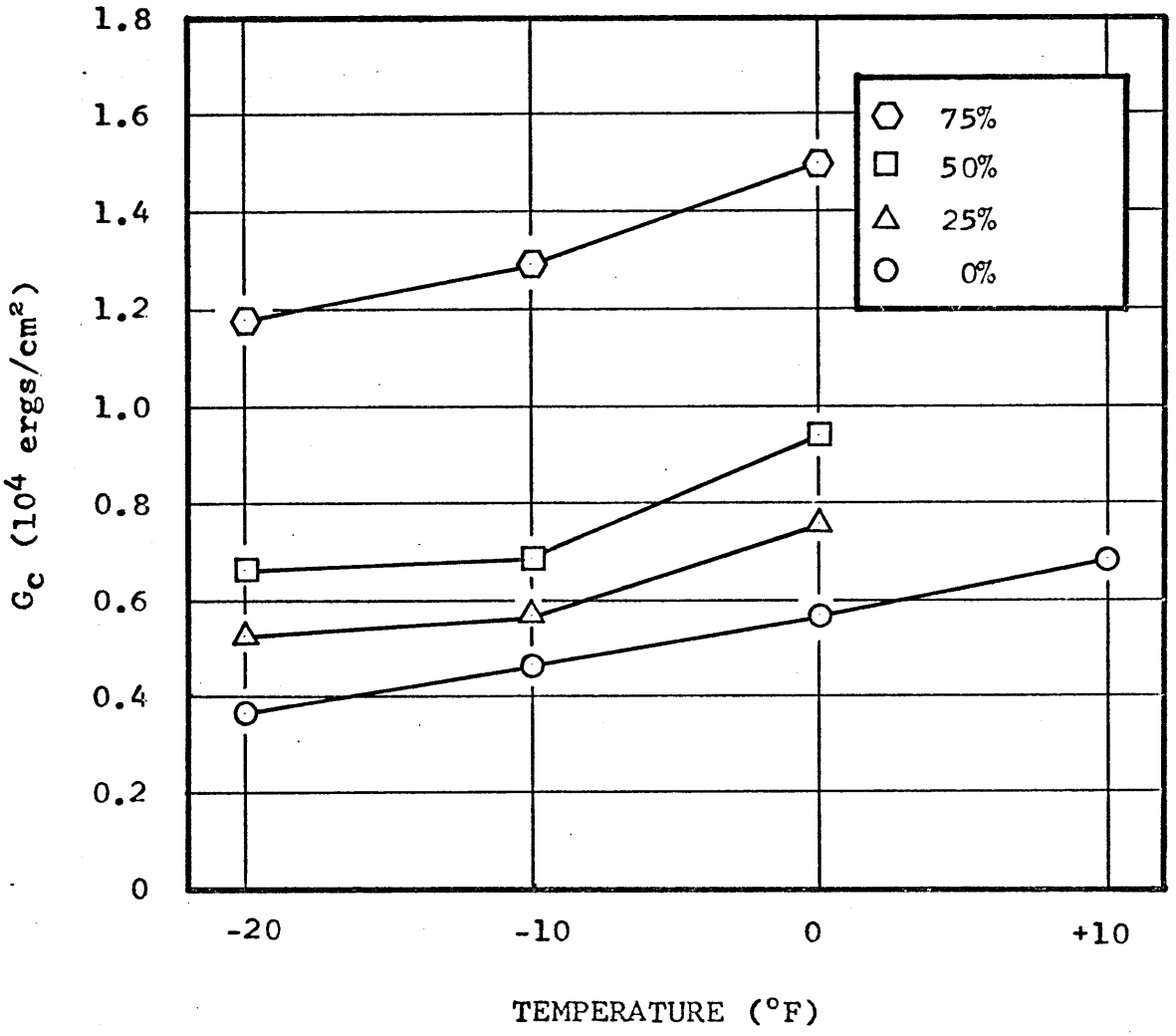

Figure 15 - G_c versus Temperature for B-3056 Asphalt mixed with Filler and Loaded at .10 in/min

and have a "gritty" texture. This is very much unlike the fracture surfaces of unfilled asphalt beams, which are generally smooth and glassy in appearance and contain such characteristic markings for glassy polymers as geometric tear lines and "river" systems, etc. (see Figure 16). Thus, it appears that in the filled beams the crack is forced to propagate around the small individual mineral particles, causing an increase in fracture surface area and subsequent increase in energy required for fracture. The fracture surface becomes so rough in some beams with large percentages of filler that the two halves of the fractured beam do not separate once the crack has propagated through the specimen. In some cases, the friction between fracture surfaces was great enough so that the beam was capable of supporting load in a fractured state. A schematic load-deflection diagram for this case is given below:

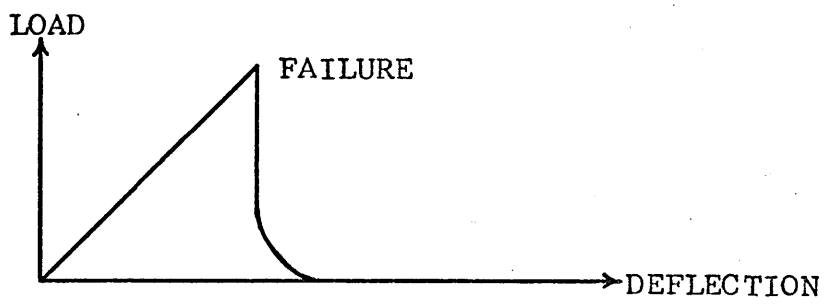

This phenomena never occurred with the unfilled asphalt beams.

A possible reason for the large increase in G_c between 50% and 75% filler, in addition to the increased number of mineral particles which serve as barriers to the crack, could be a transition from thick film to thin film behavior in the

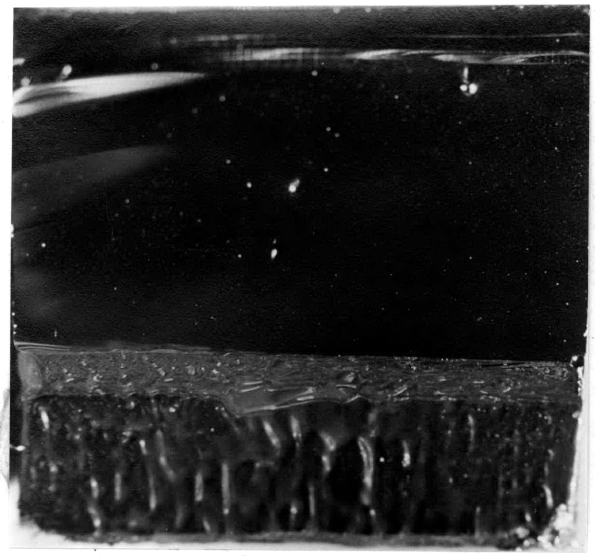

Notched B-3056
Beam

Unnotched B-3056
Beam

Notched B-2960 Beam
with 75% Filler

Unnotched B-2960 Beam
with 25% Filler

Figure 16 - Appearance of Fracture Surfaces

asphalt. The greater the number of mineral particles in an asphalt beam, the thinner the film of asphalt which surrounds each particle. As discussed by Majidzadeh (22), the amount of energy required for fracture varies with film thickness due to changes in the state of stresses in the film. In thinner films, where the asphalt is subjected to a state of triaxial stresses, the amount of energy required for fracture is expected to be higher than in thick films that are less effected by such stresses. Thin film behavior may be occurring in asphalt beams containing 75% mineral filler.

Effect of Aging

The data for both asphalts aged at 375°F for six hours is presented in Table 7. G_c is plotted versus temperature for aged B-2960 and B-3056 asphalt in Figures 17 and 18, respectively. As shown in these plots, the value of G_c decreases due to aging for both asphalts. Since aging makes asphalt behavior more non-Newtonian, and since B-3056 is initially more non-Newtonian than B-2960 asphalt, it is not unusual that aging has a greater effect on the behavior of B-2960 asphalt than on B-3056 asphalt. As easily seen in Figure 18, the effect of aging becomes less significant when beams are tested at lower temperatures.

Table 8 presents the data for aged asphalt beams tested in a silicone oil bath. As will be discussed under the next topic, testing in silicone oil reduces the measured values of

Table 7 - Data Summary for Aged Asphalts
($\dot{\gamma}$ =.10 in/min)

ASPHALT	TEMP	AGING at 375°F	E 10^7 dynes per cm^2	Pmax 10^5 dynes	Gc 10^4 ergs per cm^2
B-2960	-10°F	0 Hr.	277	6.26	1.441
		6 Hr.	286	5.11	0.928
	-20°F	0 Hr.	409	6.84	1.164
		6 Hr.	436	5.48	0.703
	-30°F	0 Hr.	550	7.46	1.033
		6 Hr.	541	5.95	0.669
B-3056	0°F	0 Hr.	481	5.15	0.564
		6 Hr.	547	4.51	0.378
	-10°F	0 Hr.	628	5.35	0.465
		6 Hr.	720	5.06	0.362
	-20°F	0 Hr.	935	5.82	0.368
		6 Hr.	870	5.37	0.341

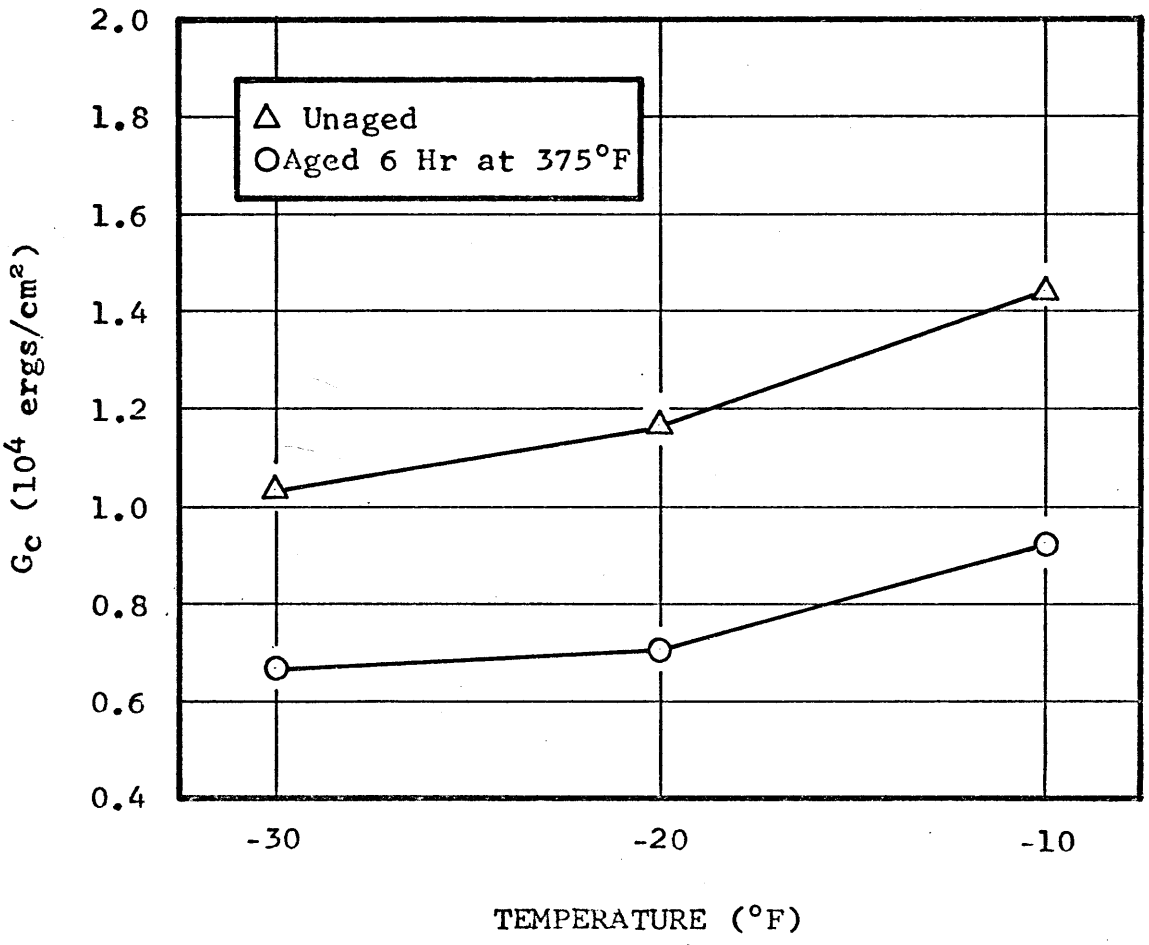

Figure 17 - G_c versus Temperature for Aged B-2960 Asphalt Loaded at .10 in/min

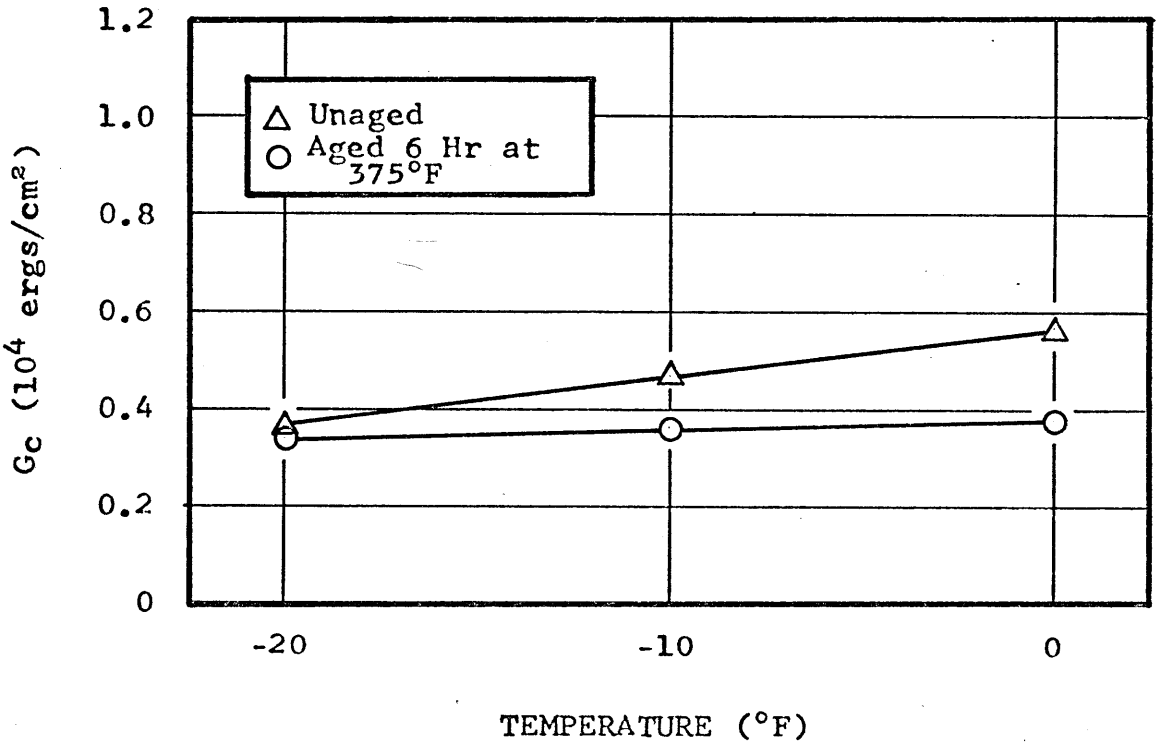

Figure 18 - G_c versus Temperature for B-3056 Asphalt Loaded at .10 in/min

G_c significantly and makes the effect of different test variables become less pronounced. Nevertheless, Figure 19, where G_c is plotted versus degree of aging for B-2960 asphalt, shows that the first three hours of aging at 375°F has the greatest effect on reducing G_c, and that the subsequent three hours of aging do not produce any significant further reduction in G_c. Figure 20, where the same is plotted for B-3056 asphalt, shows that practically no reduction in G_c can be observed for aged B-3056 asphalt when tested in silicone oil.

The reduction in G_c due to aging can possibly be explained by the changes which occur in the molecular structure of asphalt during the aging process. As the asphalt is heated at high temperatures for a period of time, oxidation occurs wherein oxygen takes hydrogen from the asphalt in the form of water and leaves unsaturated hydrocarbon molecules in the asphalt. These unsaturated hydrocarbons combine with one another to create larger molecules. Furthermore, at these high temperatures volatilization occurs wherein the lighter constituents, molecular weight less than 400, of asphalt are evaporated (21). Thus the asphaltene content of the asphalt is increased with aging (see Table 9).

However, intrinsic viscosity measurements indicate that the average molecular weight of asphalt changes very little during aging, even though the asphaltene content increases (20). It appears that both molecular buildup and breakdown must take place during aging. It has been hypothesized that aging of

Table 8 - Data Summary for Aged Asphalts Tested in Silicone Oil
($\dot{\gamma}$ =.10 in/min)

ASPHALT		TEMP	AGING at 375°F		
			0 HOURS	3 HOURS	6 HOURS
B-2960	E 10^7 dynes/cm^2	-10°F	262	432	499
		-20°F	416	549	585
		-30°F	760	762	767
	P_{max} 10^5 dynes	-10°F	3.67	3.82	3.91
		-20°F	4.19	4.11	4.00
		-30°F	5.28	4.71	4.50
	G_c 10^4 ergs/cm^2	-10°F	0.523	0.343	0.312
		-20°F	0.431	0.313	0.278
		-30°F	0.373	0.296	0.268
B-3056	E 10^7 dynes/cm^2	-1.3°F	640	600	656
		-10°F	611	735	805
		-20°F	668	770	920
	P_{max} 10^5 dynes	-1.3°F	3.75	3.62	3.70
		-10°F	3.60	3.86	3.82
		-20°F	3.71	3.73	4.02
	G_c 10^4 ergs/cm^2	-1.3°F	0.224	0.222	0.212
		-10°F	0.215	0.207	0.186
		-20°F	0.210	0.184	0.179

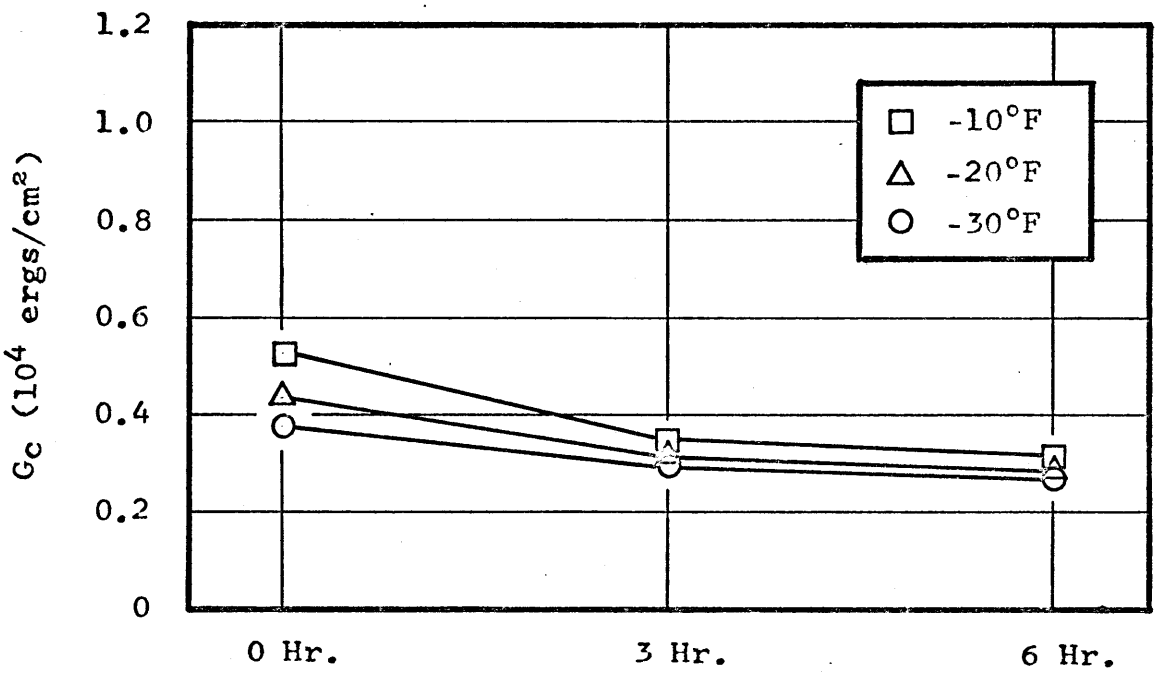

Figure 19 - G_c versus Degree of Aging for B-2960 Asphalt Tested in Silicone Oil, $\dot{\gamma}$=.10 in/min

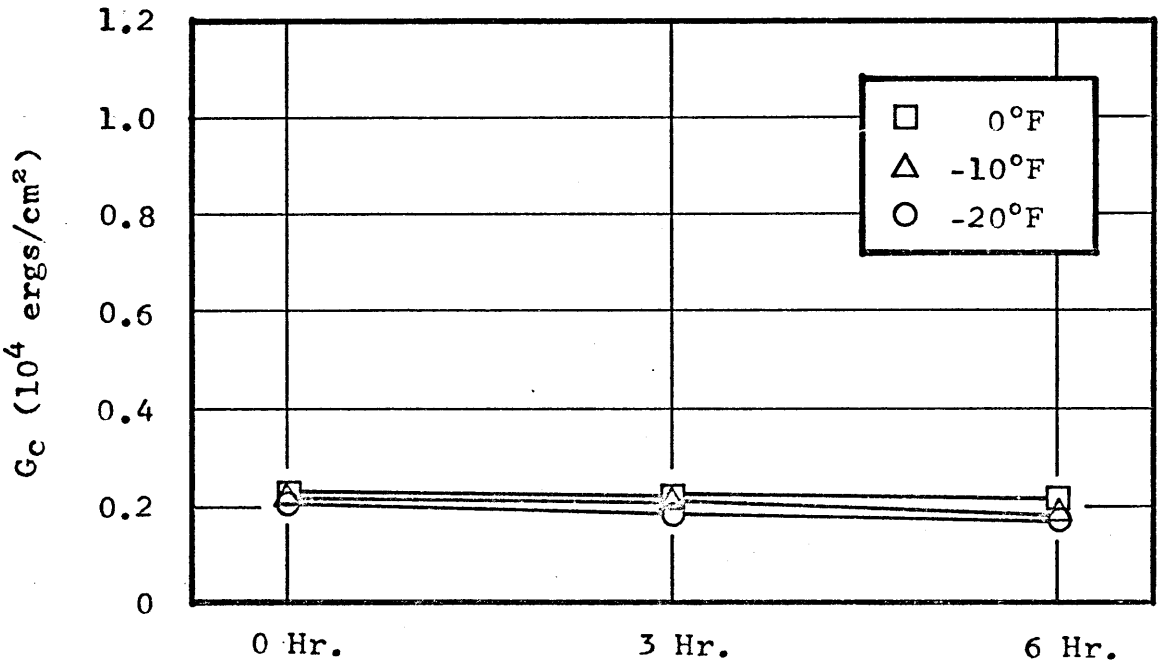

Figure 20 - G_c versus Degree of Aging for B-3056 Asphalt Tested in Silicone Oil, $\dot{\gamma}$ =.10 in/min

asphalt involves both the formation of more asphaltene units and the breakdown of the more complex units into less complex asphaltene units (20).

Table 9

Change in Asphaltene Content with Aging (20)

ASPHALT	% ASPHALTENES BASED ON WEIGHT OF SAMPLE	
	Unaged	Aged 6 Hr at 375°F
B-3056	15.88	20.03
B-2960	26.23	34.15

Since asphaltene molecules form strong association bonds throughout the structure of the asphalt, an increase in asphaltene content makes the asphalt more strongly bonded and less temperature susceptible. Polar forces also act in the association process, and their influence is determined by the degree to which suitable neighbors can be attracted. As aging decreases the size of the larger complex molecules, they become more mobile and thus more likely to assume positions favorable to polar associative forces (20). Therefore, the very slight increase in average molecular weight of the asphalt due to aging, which would tend to increase G_c, is offset by the strong associative bonds resulting from increased asphaltene content, which tend to inhibit microscopic plastic flow in the asphalt at the tip of the propagating crack and thus reduce the value of G_c. The aging process in asphalt is very similar to and

has the same effects on G_c as the process of cross-linking in other glassy polymers as discussed earlier in the literature review.

A comparison between schematic load-deflection curves for aged and unaged asphalt beams is helpful in understanding why G_c decreases for the aged beams (see Figure 21). The increased asphaltene content makes aged asphalt stiffer, as indicated by an increased value of E (slope of the load-deflection curve). However, as seen in Table 8, the failure load, P_{max}, for the aged asphalt beams is generally only equal to, or slightly greater than, P_{max} for unaged asphalt beams. Consequently, the area under the load-deflection curve, which is a measure of the energy required for fracture, is less for aged asphalt beams, and G_c decreases.

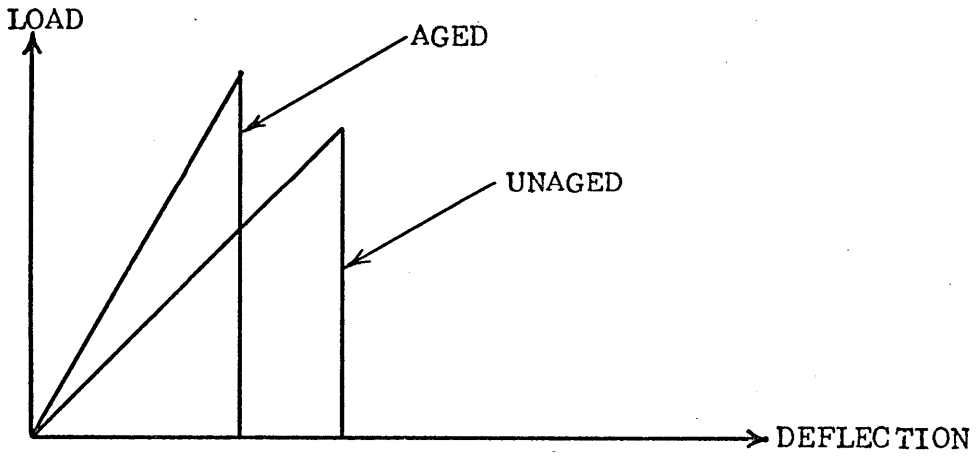

Figure 21 - Schematic Load-Deflection Curves for Aged and Unaged Asphalt Beams

Effect of Testing in Oil

The data for both asphalts tested in silicone oil is presented in Table 10. As shown in Figures 22 and 23, where the values of G_c are compared between beams tested in silicone oil and beams tested in the atmosphere for B-2960 and B-3056 asphalt, respectively, the values of G_c are decreased by approximately 33% by testing in silicone oil for both asphalts. Furthermore, the effects of test variables become less pronounced by testing in silicone oil,as indicated by the relative slopes of the curves plotted in both Figures 22 and 23 where temperature is the test variable.

This behavior can be explained by the fact that silicone oil seeps into the microcracks at the crack tip and tends to force them open. The result is an apparent decrease in fracture surface energy, and the measured value of G_c is reduced. The fracture surfaces of beams tested in silicone oil were less featured than those of beams tested in the atmosphere.

Effect of Rate of Loading

Although testing in silicone oil greatly inhibits the effects of the rate of loading the asphalt beams on the observed values of G_c, some inferences can be made by examining Figures 24 and 25. In Figure 24, G_c for B-2960 asphalt is plotted versus temperature for various rates of loading. As the strain rate is increased, the value of G_c is decreased. In Figure 25, where G_c is plotted versus rate of loading at

Table 10 - Data Summary for Asphalts Tested in Silicone Oil

ASPHALT	TEMP	STRAIN RATE in/min	E 10^7 dynes per cm^2	P_{max} 10^5 dynes	G_c 10^4 ergs per cm^2
B-2960	0°F	.05	137	3.12	0.726
		.10	158	3.33	0.715
		.20	202	3.67	0.677
	-10°F	.05	166	2.98	0.546
		.10	262	3.67	0.523
		.20	329	3.95	0.483
	-20°F	.05	384	4.16	0.458
		.10	416	4.19	0.431
		.20	510	4.48	0.403
	-30°F	.05	666	5.06	0.392
		.10	760	5.28	0.373
		.20	800	5.39	0.371
B-3056	+10°F	.05	351	3.14	0.287
		.10	419	3.20	0.250
		.20	504	3.46	0.243
	- 1.3°F	.05	608	3.02	0.152
		.10	640	3.75	0.224
		.20	785	4.01	0.208
	-10°F	.05	526	3.51	0.238
		.10	611	3.60	0.215
		.20	702	3.73	0.203
	-20°F	.05	580	3.62	0.231
		.10	668	3.71	0.210
		.20	779	3.88	0.196

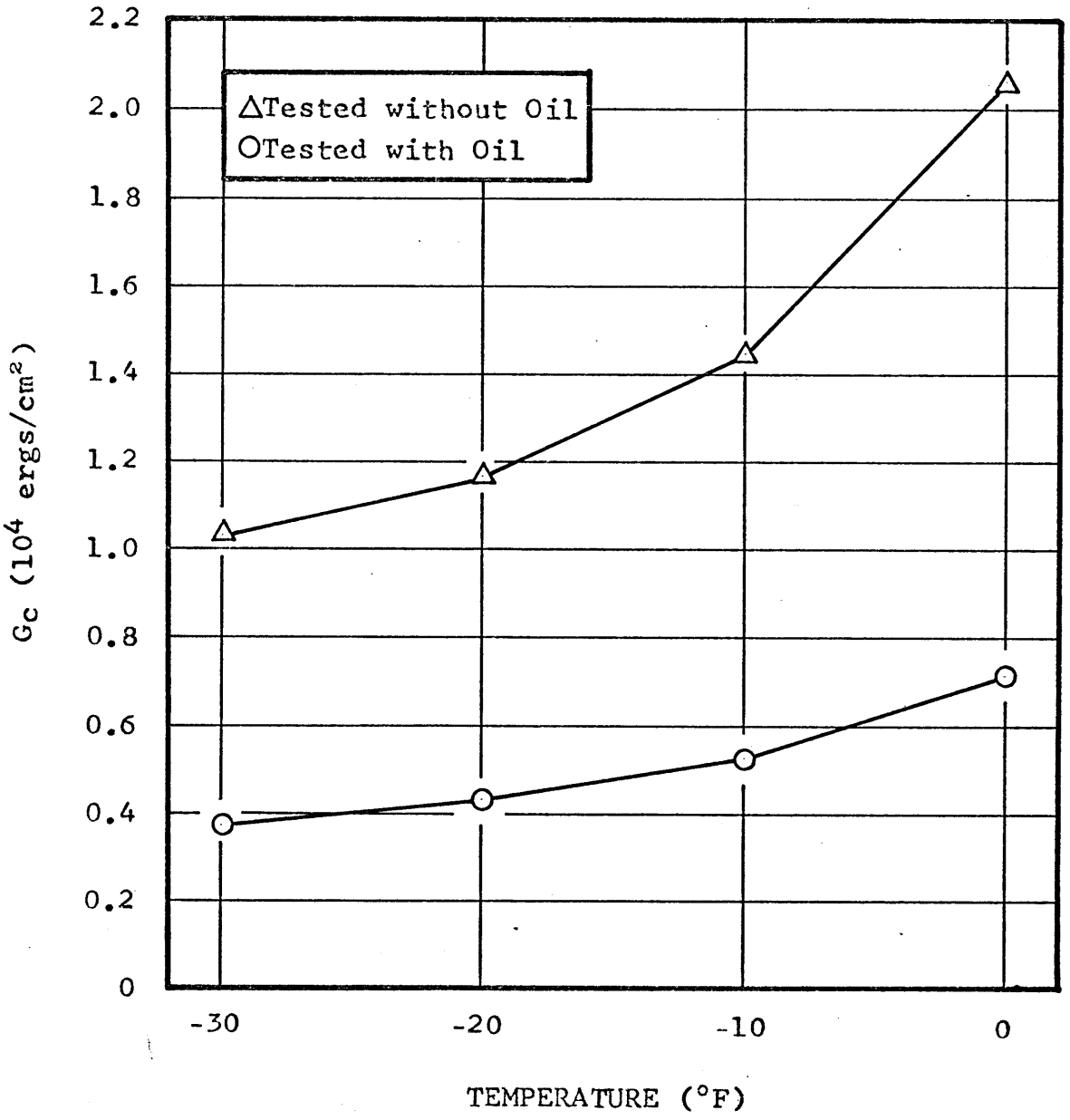

Figure 22 - G_c versus Temperature for B-2960 Asphalt Tested with and without Silicone Oil, $\dot{\delta}$=.10 in/min

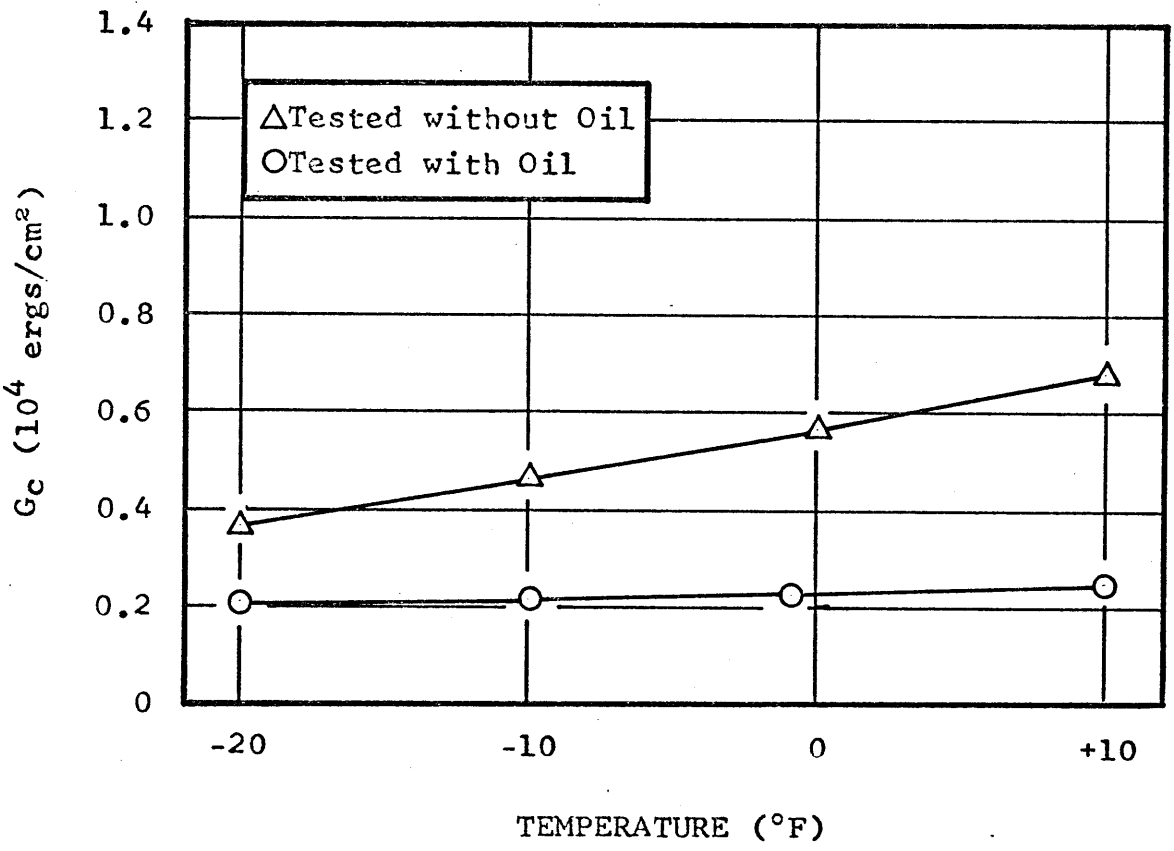

Figure 23 - G_c versus Temperature for B-3056 Asphalt Tested with and without Silicone Oil, $\dot{\delta}$=.10 in/min

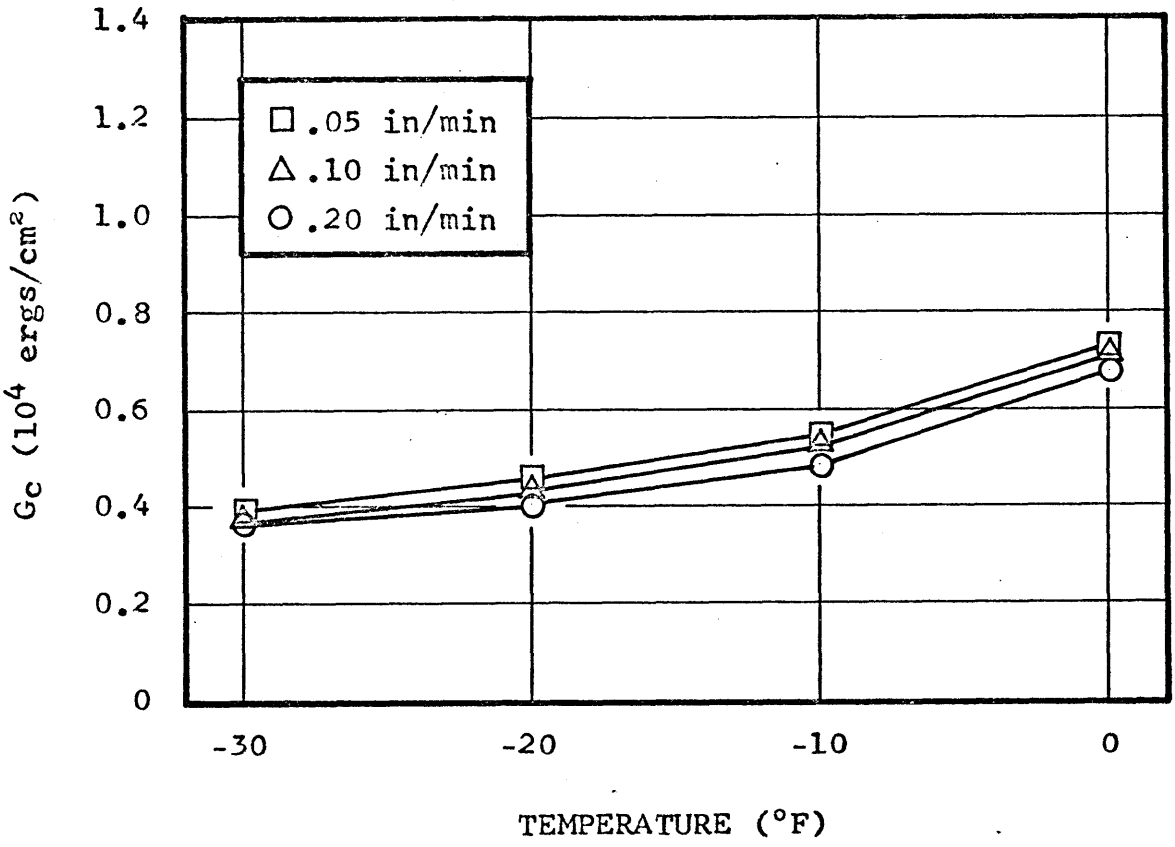

Figure 24 - G_c versus Temperature for B-2960 Asphalt Tested in Silicone Oil at Various Rates of Loading

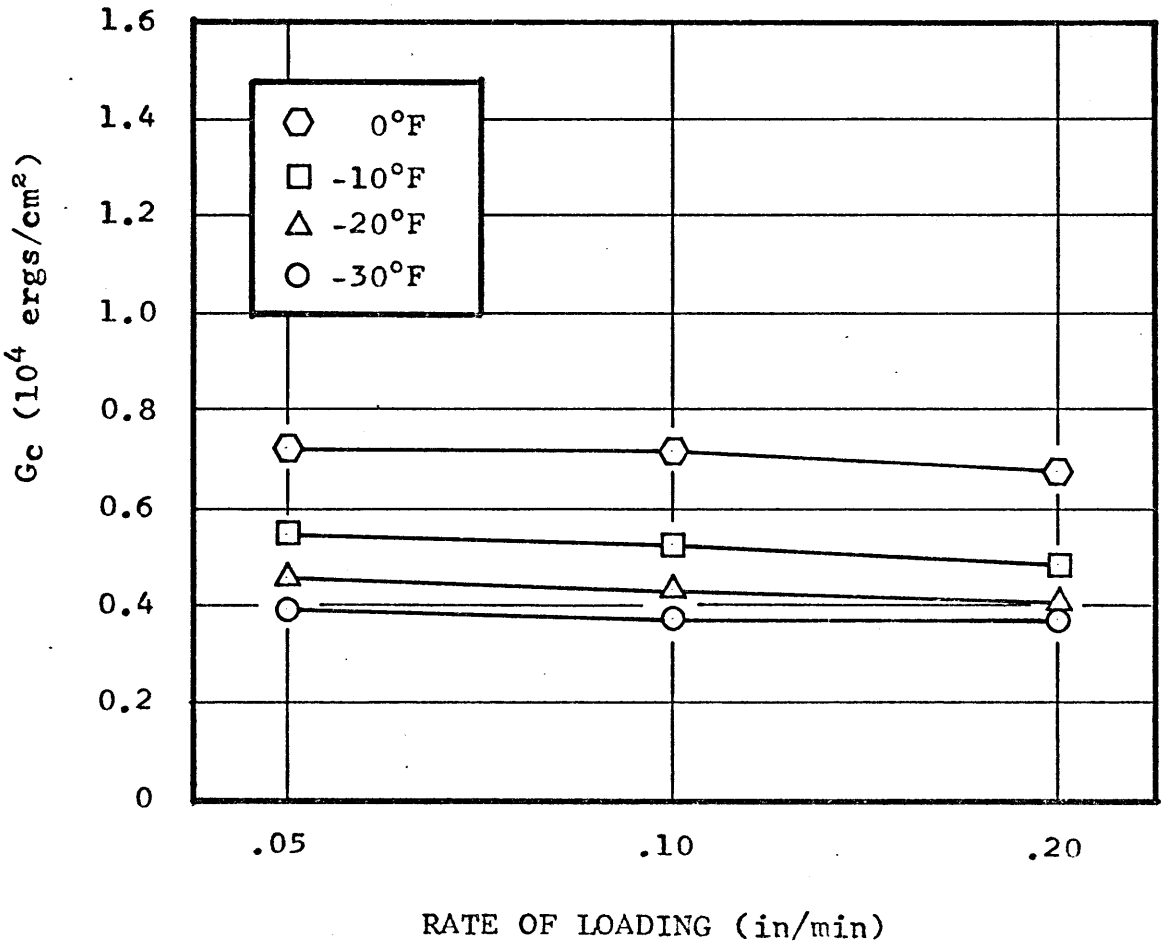

Figure 25 - G_c versus Rate of Loading for B-2960 Asphalt Tested in Silicone Oil

various test temperatures for B-2960 asphalt, it is shown that the effect of increasing the strain rate on the values of G_c becomes practically negligible at the lower temperatures.

The decrease in G_c with increasing strain rates seems reasonable since the faster the specimen is loaded and the faster the crack is forced to grow, less time is available for microscopic inelastic flow processes at the tip of the crack which contribute greatly to the fracture surface work. Consequently, less energy is required for fracture, and G_c decreases.

CONCLUSIONS

In this study, tests on notched beams are used for the determination of the critical strain-energy release rate for two paving asphalts at various conditions of temperature, percentage of mineral filler, aging, test environment, and rate of loading. From the results of this study, the following conclusions are drawn:

1. The Griffith theory of brittle fracture can be applied to study the fracture behavior of asphalts at sufficiently low temperatures.
2. The addition of mineral filler significantly increases the fracture toughness of asphalt as indicated by a threefold increase in the value of the critical strain-energy release rate.
3. Aging causes asphalt to become stiffer as indicated by increased values of the modulus of elasticity; however, the fracture toughness of aged asphalt is less than that of unaged asphalt.
4. The fracture behavior of asphalt can be related to the fracture behavior observed in other polymeric materials.
5. Testing in a silicone oil constant temperature bath greatly reduces the measured values of the critical strain-energy release rate and causes the effects of different test variables to be less pronounced.

The results of this study also indicate the need for, and the possibilities of, further investigation in the following areas:

1. The study should be extended to include a wider range of temperatures below the glass transition region of the asphalts tested.
2. The addition of mineral filler in aged asphalts should be investigated.
3. The possibility of mixing rubber with asphalt and asphaltic mixtures to improve fracture toughness should also be investigated.
4. After sufficient data has been determined for the fracture behavior of asphalt, an attempt should be made to establish practical specifications for asphalt fracture considerations in pavement design requirements.

REFERENCES

1. Vallerga, B. A., "On Asphalt Pavement Performance", Proceedings, Association of Asphalt Paving Technologists, Volume 24, 1955.

2. Finn, F. N., "Factors Involved in the Design of Asphalt Pavement Surfaces", Highway Research Board Report HR 1-8, March, 1966.

3. Marsh, J. D., Fracture of Asphalt, S.M. Thesis, M.I.T., 1966.

4. Griffith, A. A., "The Phenomena of Rupture and Flow in Solids", Philosophical Transactions, Royal Society of London, Series A, Volume 221, 1920.

5. Griffith, A. A., "The Theory of Rupture", First International Congress of Applied Mechanics, Delft, 1924.

6. Inglis, C. E., "Stresses in a Plate Due to the Presence of Cracks and Sharp Corners", Transactions, Institute of Naval Architects, Volume 55, 1913.

7. Orowan, E., "Fracture and Strength of Solids", Reports on Progress in Physics, Volume 12, 1949.

8. Orowan, E., "Fundamentals of Brittle Behavior in Metals", Fatigue and Fracture of Metals, (M.I.T. Symposium, June, 1950). John Wiley and Sons, Inc. New York, 1950.

9. Irwin, G. R., "Fracture Dynamics", Fracturing of Metals, American Society of Metals, Cleveland, Ohio, 1948.

10. Irwin, G. R., "Relation of Stresses Near a Crack to the Crack Extension Force", Proceedings, Ninth International Congress of Applied Mechanics, Paper No. 101 (11), Brussels, 1956.

11. Irwin, G. R., "Fracture Mechanics", First Symposium on Naval Structural Mechanics, Stanford University, August, 1958.

12. Berry, J. P., "Brittle Behavior of Polymeric Solids", Fracture Processes in Polymeric Solids, Interscience, New York, 1964.

13. Broutman, L. J., and McGarry, F. J., "Fracture Surface Work Measurements on Glassy Polymers by a Cleavage Technique", Journal of Applied Polymer Science, Volume 9, 1965.

14. Tetelman, S. S., and McEvily, A. J., Fracture of Structural Materials, John Wiley & Sons, Inc., New York, 1967.

15. Berry, J. P., "Fracture Topography", Fracture Processes in Polymeric Solids, Interscience, New York, 1964.

16. Boyer, R. F., "The Relation of Transition Temperatures to Chemical Structure in High Polymers", Rubber Chemistry and Technology, Volume 36, December, 1963.

17. Schmidt, R. J., and Santucci, L. E., "A Practical Method for Determining the Glass Transition Temperature of Asphalts and Calculation of Their Low Temperature Viscosities", Proceeding, Association of Asphalt Paving Technologists, Volume 35, February, 1966.

18. Kaplan, M. F., "Crack Propagation and the Fracture of Concrete", Proceedings, Journal of the American Concrete Institute, Volume 58, November, 1961.

19. Winnie, D. H., and Wundt, B. M., "Application of the Griffith-Irwin Theory of Crack Propagation to the Bursting Behavior of Discs, Including Analytical and Experimental Studies", Transactions, ASME, Volume 80, 1958.

20. Moavenzadeh, Fred, and Stander, R. R., Durability Characteristics of Asphaltic Materials, Report No. EES 259-1, Ohio State University, Columbus, Ohio, June 1966.

21. Monesmith, Carl L., Asphalt Paving Mixtures - Properties, Design, and Performance, Course Notes, The Institute of Transportation and Traffic Engineering, University of California, Berkeley, 1961.

22. Majidzadeh, K., Tensile Properties of Asphalts in Thin Films, Ph.D. Thesis, University of Illinois, Urbana, Illinois, 1963.

A P P E N D I C E S

DEFINITION OF SYMBOLS

a = interatomic spacing

c = notch depth (crack length)

c_n = 1/2 h

d = over-all depth of beam

h = net depth of beam at notch = d - c

ℓ = span length

n = constant

A = constant

E = modulus of elasticity

G = strain-energy release rate

G_c = critical strain-energy release rate

I = moment of inertia of beam

I_n = moment of inertia of notched cross section of beam

M_b = mid-span bending moment

M_v = molecular weight

P = applied load

P_{max} = load required to fracture a notched specimen

T = energy required for the formation of the fracture surfaces of a system

T_g = glass transition temperature

U = elastic strain-energy of a system

W = T - U

γ = surface energy of the material per unit area

γ_p = fracture surface work of the material per unit area

DEFINITION OF SYMBOLS (Continued)

$\dot{\gamma}$ = strain rate (rate of loading)

ν = Poisson's ratio

ρ = radius of curvature at crack tip

σ = stress

σ_c = cohesive strength of material

σ_m = maximum stress at the crack tip

σ_n = nominal stress at the crack tip

τ = shear stress

LIST OF FIGURES

LIST OF FIGURES (Continued)

LIST OF TABLES